TRABAJOS FIN DE GRADO

Universidad de Jaén

Escuela Politécnica Superior de Jaén

Simulación fluidodinámica de Equipos para el Ensayo de Catalizadores tipo automoción mediante Ansys Fluent

Kaouthar Ben Said

Grado: Grado en Ingeniería Mecánica

Departamento
Ingeniería Mecánica y Minera

Fecha: 03/07/2024

CREA

Universidad de Jaén
Escuela Politécnica Superior de Jaén
Departamento de Informática

Profesoa FRANCISCA MARIA GUERRERO VILLAR y Profesor FRANCISCO MORAL PULIDO, tutor del Proyecto Fin de Carrera titulado: Simulación fluidodinámica de Equipos para el Ensayo de Catalizadores tipo automoción mediante Ansys Fluent, que presenta Kaouthar Ben Said, autoriza su presentación para defensa y evaluación en la Escuela Politécnica Superior de Jaén.

Jaén, JULIO de 2024

El alumno: Los tutores:

Kaouthar Ben Said

Profesora Francisca Maria Guerrero Villar

Profesor Francisco Moral Pulido

Table of content

List of Figures

List of Tables

Introduction

The automotive industry faces a critical challenge; balancing efficiency and environmental responsibility. Vehicular emissions continue to threaten air quality, prompting a relentless pursuit of cleaner technologies. This project investigates the critical role of airflow parameters in automotive design. These parameters directly influence both a vehicle's performance and its environmental impact. By optimizing airflow, engineers can achieve significant strides toward cleaner and more efficient transportation.

Chapter 1 sets the stage by exploring wind tunnels. It examines their role in evaluating fluid-dynamic parameters around objects, highlighting the various wind tunnel types and their functionalities.

Chapter 2 focuses on catalytic converters. It explores how these devices function and the factors that govern their effectiveness, emphasizing the role of airflow parameters in optimizing their performance.

Chapter 3 delves into the realm of Computational Fluid dynamics (CFD) simulations. It explores the critical step of mesh generation, emphasizing its impact on the accuracy of fluid-dynamic simulations. This chapter discusses various meshing methods and the importance of mesh quality for accurately capturing airflow patterns.

Chapter 4 details the specific materials and methods employed in the research conducted for this project. The chapter outlines the selection of materials, the experimental setup and the data collection procedures undertaken to achieve the research objectives.

Chapter 5 presents the results obtained from the research and delves into a discussion of their significance. This chapter aims to contribute to a deeper understanding of their eventual influence.

The concluding chapter summarizes the key findings of the research and their broader implications.

Chapter I
Wind Tunnels

Introduction

The wind tunnel is imperative to the development of modern aircraft. They are very favorable as they reduce the money and time consumption of making prototypes and testing them in real-world conditions. Presently, a very crucial procedure in the creation of a high-performance airplane design is to analyze its characteristics in a wind tunnel.

Thus, the primary practical purpose of wind tunnels is to obtain information from which aeronautical designers can rectify and develop more powerful airplanes.

Designing an advanced aircraft is highly challenging. For this reason, many varieties of data are required before making a perfect design. Apart from aircraft, wind tunnels are also useful for any device that involves interaction with flow. For instance, it is mandatory to examine the lift properties, drag properties, stability, and controllability of the device in a wind tunnel.

In this chapter, we will establish a solid foundation for the research by examining the knowledge about wind tunnels. Hence, we will start with a broad definition of this equipment and then go over its primary aspects.

I.1. Wind Tunnels

A wind tunnel is an equipment used by researchers and engineers to test and characterize the aerodynamics of an object. It helps with visualizing the wind's interaction with objects (see Figure 1). The test material remains stationary, and a rapid airflow inside the tunnel makes it seem as though it is moving. The object is generally a scale model but some wind tunnels help with testing full-size products. The wind tunnels are designed to generate airflows at various speeds through a test section. The speed of air flowing is usually expressed in terms of the speed of sound. The tests are necessary to provide more data for the engineers, such as pressure, velocity, temperature, density, and aerodynamic forces like lift and drag. Eventually, they analyze this data to make a safe, optimized, and refined product to reach the desired results.

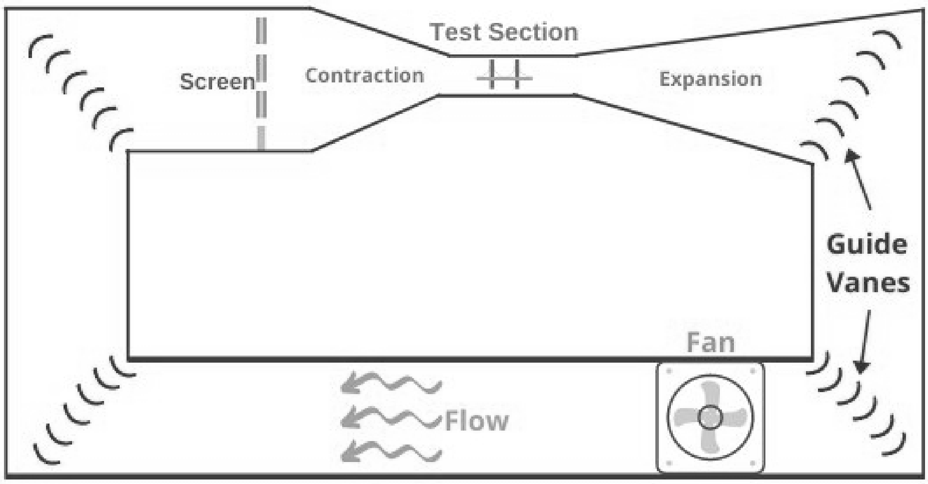

Figure 1: Open circuit wind tunnel [1]

I.2. How wind tunnels work

Inside the tunnel, powerful fans create a flow of air, the conditions the object would encounter in real-world scenarios. The object is fixed in the tunnel. The air movement around that stationary object simulates the airflow that would occur if the object were in motion. Wind tunnels are equipped with sensors and instruments that help engineering gain data regarding an object’s interaction with the wind. [3]

Testing of a Model

The analysis of the object is carried out in the test section. A powerful fan generates air that moves around the fixed object. A study of the effects of the air on the object is now executed through the use of different instruments and sensors in the test section. Thus, we can measure pressure, aerodynamic forces, and many other characteristics around the object.
The major types of tests inside the test section are:

Measurement of forces and moments

The forces and moments measurements are performed using a specialized machine called a force balance. It also serves as a support for the object. After the test, we need to post-test process or perform data reduction to the measured forces to correct any influences of factors like Mach number or Reynolds number, thus ensuring the accuracy of the results.

Pressure measurement for performance evaluation

Pressure measurement is carried out by employing small sensors called pressure taps to obtain data on the pressures. These taps reveal how air interacts with the model by measuring pressure variations. Ideally, they should be placed everywhere. However, by placing enough taps, it is possible to directly calculate the total lift and drag forces acting on the model, giving insights into its aerodynamic performance.

Visualization of the flow

Flow visualization methods, such as laser sheets, free stream smoke, or surface oil flow, offer diagnostic insights in some tests. These techniques assume that the movement of the medium mirrors the flow being studied. For low-speed flows, surface oil or tufts can be employed to indicate flow direction around the model surface.

Pressure Drops and Boundary Layer Growth

When the length of the hydraulic test section exceeds three times its hydraulic diameter, it can cause excessive formation and growth of the boundary layer which will probably be causing a separation of the flow at the exit of the test section and into the diffuser. As the boundary layer grows, there is a significant decrease in static pressure along the length of the test section.

I.3. Types of wind tunnels / Classification

I.3.1. Based on the average speed in the test section

I.3.1.1. High-speed wind tunnel: average speed in the test section > 100 m/s

High-speed wind tunnels are used to test objects at high velocities that may exceed the speed of sound. Shock waves may occur at this type of speed. For this reason, it is crucial to make design adjustments for some key components to accommodate these conditions.

I.3.1.2. Low-speed wind tunnel: average speed in the test section < 100 m/s

These tunnels are designed to study the aerodynamics of objects at low velocities, generally below the speed of sound. They play a key role in industries such as automotive, civil engineering, and sports. [4]

I.3.2. Based on Mach number regimes

The Mach number represents the ratio of the speed of an object to the speed of sound in the surrounding environment. [2]

Based on the desired flow speed in the test section, the wind tunnels are divided into :

a. Subsonic wind tunnels (Mach < 0.8)

Subsonic wind tunnels are the most common type. They operate at speeds below the speed of sound. They serve numerous applications such as the testing of aircraft, automobiles, buildings, and sports equipment.

b. Transonic wind tunnels (0.8 < Mach < 1.2)

Transonic wind tunnels are designed to generate airflow at speeds near or slightly above the speed of sound. They are common in the aircraft industry, generally used for testing airfoil designs, engine components, and missiles.

c. Supersonic wind tunnels (1.2 < Mach < 5)

Supersonic wind tunnels operate at speeds faster than the speed of sound. They can be used to investigate the behavior of high-speed aircraft, spacecraft and military aircraft.

d. Hypersonic wind tunnels (Mach > 5)

Hypersonic wind tunnels are designed to operate at extremely high speeds, exceeding the speed of sound. They are extensively used for testing rockets and space vehicles. They require specialized facilities to generate and control airflow at such high velocities.

I.3.3. Based on tunnel design

Depending on the shape and how the air is circulated, wind tunnels can be classified in two categories: Open-circuit wind tunnels and closed-circuit wind tunnels.

a. Open-circuit

Open wind tunnels have open ends on both sides of the test section, gathering air from the environment where it is located. It is a type of low-speed wind tunnel. Air is drawn from the surroundings into the tunnel inlet. The fan is placed near the outlet of the tunnel.

The open circuit wind tunnel is often the simplest and most affordable to build. In addition to their low cost open-circuit wind tunnels are also advantageous because they occupy less space and continuously bring in fresh fluid. There is also no more need to use corners and long diffusers. However, it requires high power to drive the wind tunnel because of the loss of energy in the outflowing air. Another drawback is that it is noisy and generates relatively poorer flow quality. For scaled building models, the open-circuit wind tunnel is selected for studying airflows (see Figure 2). This prevents blockage effects and will accurately represent real-world conditions. An open-circuit wind tunnel facilitates such a requirement because the airflow has more space to move around the model. [2]

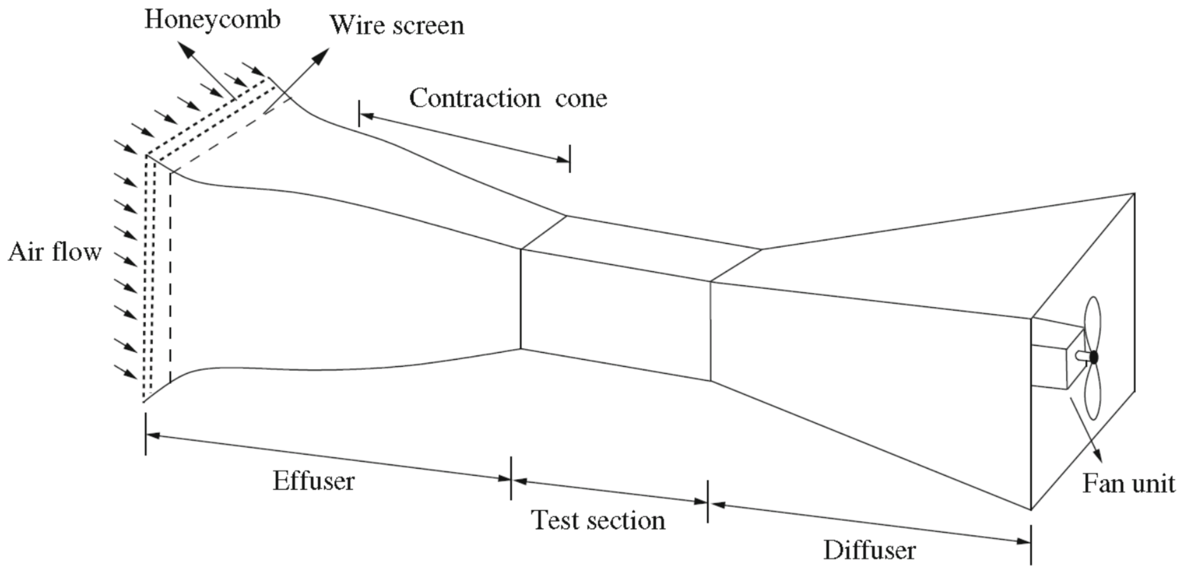

Figure 2 : Diagram of an open-circuit low-speed wind tunnel [4]

b. Closed-circuit

Closed-circuit tunnels use a self-contained circuit that recirculates air within the tunnel through the test section. The same air is circulated in a closed loop within the wind tunnel. Thus, exhaust flow is directly returned to the tunnel inlet. The tunnel is not open to the test environment surrounding the apparatus, so the same air is circulated over and over again. [5]

Closed circuit tunnels retain a fixed mass of air and circulate flow in a loop through the various wind tunnel components (see Figure 3). While having additional construction expenses, they have lower operating costs than open-circuit facilities under similar operating conditions. In fact, it consumes less energy and if it is designed carefully, it will generate a controlled, high-quality flow inside the test section. [2]

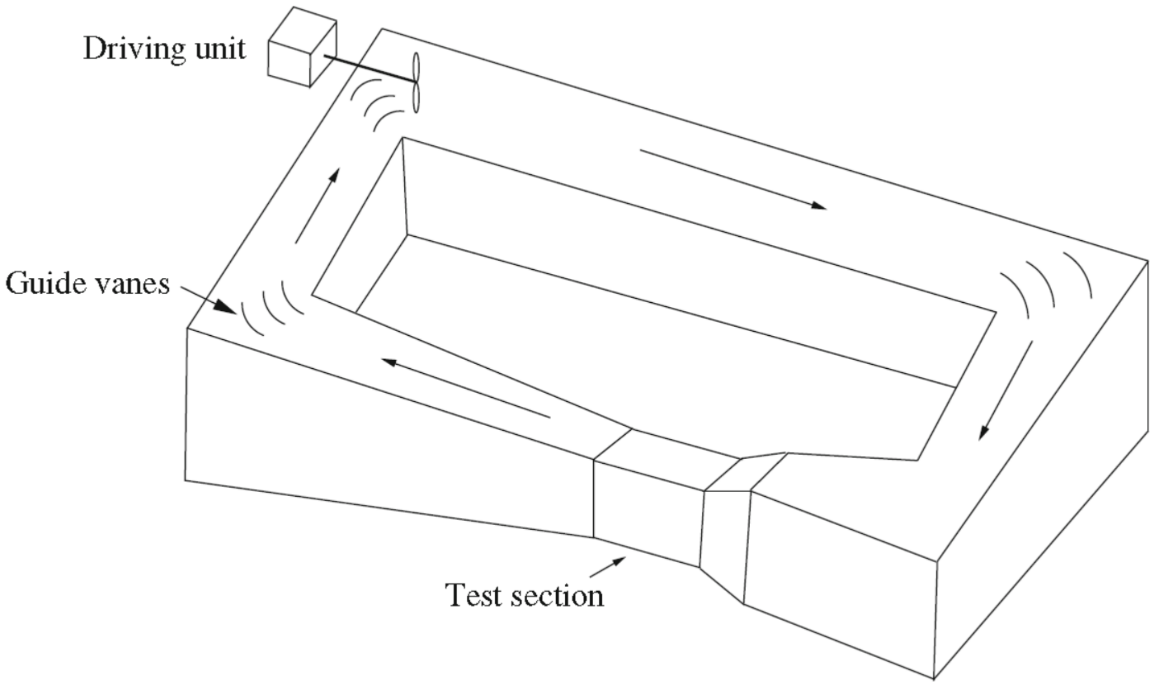

Figure 3: Diagram of a closed-circuit wind tunnel [4]

I.4. Components and instrumentation of Wind Tunnels

I.4.1. Settling Chamber

The settling chamber has the largest cross-section in the wind tunnel. It is located before the test section. It contains honeycombs and screens. The air is settled; it's slowed and smoothed out in order to reduce turbulence and create a steady and uniform airflow in the test section.

The main purpose of the settling chamber is to make the flow become straight, less turbulent, and more uniform. Its important components are honeycomb and screens. [2]

I.4.1.1. Honeycomb

Air can enter to the tunnel from any direction, but only axial flow is desired. Honeycombs are used to straighten the flow in the axial direction and to reduce the non-uniformity of the flow (see figure 4). They help to cease the tangential velocity of the airflow caused by the axial fan. It also reduces the turbulence level of the airflow. The length of the honeycomb should be 5-10 times of the cell diameter. The shape of the honeycomb cell is usually hexagonal and is generally made of aluminum. [7]

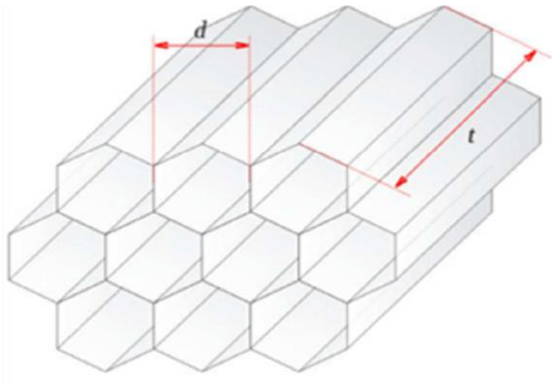

Figure 4: Honeycomb structure [5]

I.4.1.2. Screen

Screens are used to regulate and control the airflow before it enters the test section. Their main role is to reduce turbulent intensity in the flow and to prevent any unwanted objects from entering the tunnel. The number of screens depends on the desired flow quality requirements.

Screens help to increase the uniformity of the airflow as passing through a screen, faster flows have more pressure drop than slower ones. The frontal area of the screen should not be more than 40% of the cross-sectional area of the settling chamber to ensure flow stability.

I.4.2. Contraction Cone

The contraction cone is located between the settling chamber and the test section (see Figure 5). It serves to both accelerate the flow at the test section inlet and to lower inconsistencies in the uniformity of the flow. The contraction ratio, symbolized by C, is the most important parameter in determining these effects. Large contraction ratio and short contraction length are generally more desirable as they reduce cross-sectional velocity variation and maintain flow uniformity. A large contraction ratio means that the cross-sectional area decreases significantly from the settling chamber to the test section. This reduction causes the airflow velocity to increase as it moves from the settling chamber to the test section. [8]

Contraction is the most important component of a wind tunnel because it strongly affects the quality of the airflow in the test section.

As the flow area reduces, the flow speeds up through the contraction. Three main parameters of a contraction are contraction ratio (ratio between area at inlet and outlet), wall shape, and contraction length. They are computed carefully so that there is no flow separation inside the contraction. The thickness of the boundary layer at the outlet is minimized. On the other hand, the contraction length should be as short as possible for cost and space savings. [7]

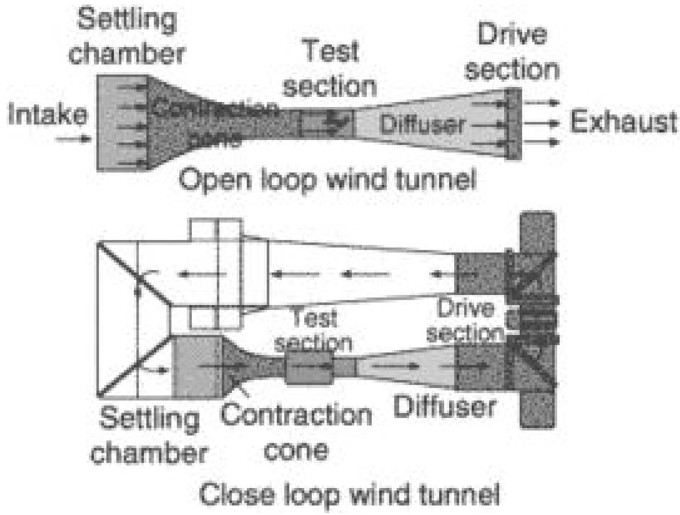

Figure 5: The contraction cone [9]

I.4.3. Test Section

The test section is the chamber in which measurements and observation are made. The test sections should be long enough that the flow disturbances resulting from contraction or screens are sufficiently damped before reaching the test object. Working section design is dependent on the requirement of the individual experimenter. However, care should be taken not to make this section too long as this will lead to detrimental boundary layer growth which can separate while entering the exit diffuser and can create a power loss. It is the basic element of a wind tunnel on which all other designs are generally made. All the aerodynamic models are mounted in the test section when the tunnel is operated with the desired flow velocity. Various shapes for the test section are considered for constructing the wind tunnel; hexagonal, octagonal, rectangle, etc. The test section is generally designed based on utility and aerodynamic considerations since the cost of construction depends on the test section area. The length of the test section is mostly equal to the major dimension of the cross-section of the same or twice. In addition, the test section should also be provided with facilities as per the testing requirement. The test section velocity is generally specified as a percentage variation from the average of the cross-section. [3]

I.4.4. Diffuser

A diffuser is a gradually expanding passage following the test section in which the flow speed decreases and the pressure rises (see Figure 6). It is a duct with an increase in area attached downstream of the test section. It connects the inlet section and the settling chamber. The air must move smoothly out of the test section. In fact, if the airflow were to exit the tunnel abruptly, it could create turbulence that interferes with the data collected during testing. So, this geometry is made to decrease the flow velocity and increase in pressure. The diffuser helps reduce energy losses in the wind tunnel system by recovering some of the kinetic energy from the high-speed airflow in the test section. The flow through a diffuser depends on its geometry defined by the area ratio, diffuser angle, and cross-sectional shapes. It is required that there is no flow separation inside this section. [3]

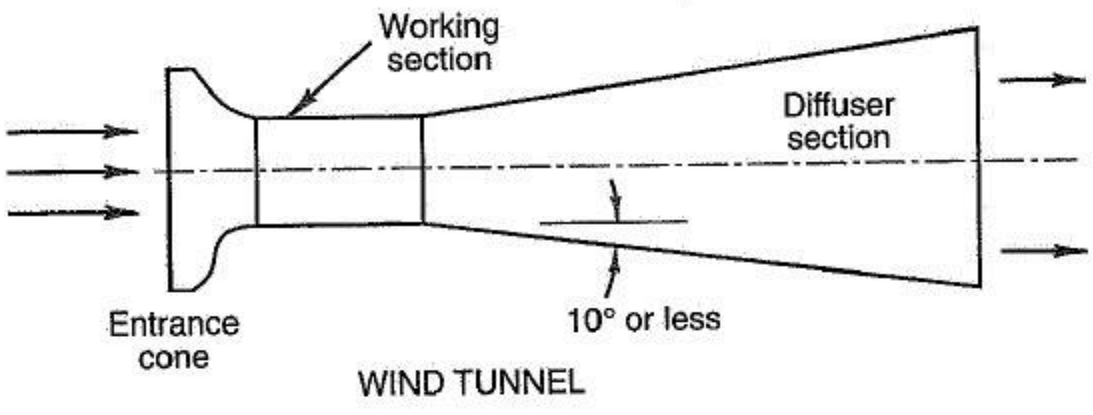

Figure 6: Wind tunnel test on diffuser angle [10]

I.4.5. Instrumentation

Instrumentation plays an imperative role in wind tunnel testing. The accuracy of experimental results depends not only on the quality of the tunnel but also on the performance of the measuring equipment. It is often important to measure the pressure distribution on the model surface and also the overall forces and moments acting on the model. Velocity in general can be calculated from pressure and need not be measured directly. We might also need to directly measure fluctuations in the velocity field in turbulent flow. Sometimes it may also be necessary to make a direct measurement of skin friction coefficient. To measure those quantities suitable instrumentation is necessary. They can be classified as two types, namely, mechanical and electronic. Examples of mechanical-type instruments are liquid-level manometers for pressure measurement and wind tunnel mechanical balances for measurement of overall forces and moments. However, such instrumentation lacks fast response and a high data acquisition rate is required for unsteady and transient measurements. Electronic instrumentation is therefore necessary to meet such requirements. A typical electronic measurement system may comprise of transducer or sensor, a signal conditioner, and a data acquisition system. The transducer detects the physical quantity (the pressure or force) being measured and transmits an electrical signal proportional to the signal conditioner. Next, the signal is amplified, filtered, and prepared for the data acquisition system by the signal conditioner. The data acquisition system might consist of an oscilloscope, digital display unit, PC, etc.

I.5. Govering Aerodynamic Equations

Wind tunnels rely on a foundation of mathematical relationships to create controlled airflows for aerodynamic testing.

In this part, the overall basic equations upon which most theoretical wind tunnel design calculations are based will be described. [7]

Continuity Equation

The continuity equation ensures a constant mass flow rate of air throughout the wind tunnel, even when the cross-sectional area changes.

$$\frac{\partial \rho}{\partial t} + \nabla \bullet (\rho \overline{V}) = 0$$

Where :

$\partial \rho$ = *change in fluid density*

∂t = *change in time*

∇ = *Divergence*

$\bullet$ = *Dot Product*

ρ = *Fluid density*

$\overline{V}$ = *Fluid velocity vector*

Incompressible Flow Assumption for Low-Speed Applications

For low-speed applications, a speed less than 0.3 Mach, the fluid is incompressible and simplifies the continuity equation.

Since density (ρ) is assumed constant, the equation reduces to :

$$\frac{\partial \rho}{\partial t} = 0$$

$$\nabla \bullet V = 0$$

Where :

ρ = Fluid density

V= Average velocity of the fluid

∂t = change in time

∇ = Divergence

• = Dot Product

Simplification for Average Two-Dimensional Flow Using Eulerian Perspective

$$Q_1=Q_2$$

$$A_1V_1=A_2V_2$$

Where :

A= Cross-sectional area

V= Average velocity of the fluid

Q= $\rho . V =$ Mass Flow

By applying Newton's Second Law of Motion to an elemental mass concerning an internal frame of reference with an ideal fluid under steady-state conditions in a uniform velocity field the classical Bernoulli Equation is derived. The Bernoulli Equation gives an estimate of the overall velocity pressure relationships throughout the low-speed wind tunnel system; by incorporating frictional and local losses into the Bernoulli Equation (Equation 3-7) it can give estimations of the overall system performance and specific pressures can be conducted.

Bernoulli Equation

In a wind tunnel, this equation helps us understand the relationship between changes in airflow speed and the resulting pressure variations around the object being tested. This principle is fundamental for analyzing aerodynamic forces like lift and drag.

$$p_1 + \frac{1}{2}\rho V_1^2 + Z_1 = p_2 + \frac{1}{2}\rho V_2^2 + Z_2$$

A modified version of the equation is necessary to account for real-world energy losses due to friction and sudden changes in direction. The term h_f will be representing the frictional and local losses.

Bernoulli Equation with Added Frictional and Local Losses

$$p_1 + \frac{1}{2}\rho V_1^2 + Z_1 - h_f = p_2 + \frac{1}{2}\rho V_2^2 + Z_2$$

Where :

p= Pressure

ρ= Fluid density

V= Average velocity of the fluid

Z= Elevation above datum

h_f *= The sum of Frictional and Local Losses*

For any fluid flow through a system, the loss coefficients for each section can be calculated. These loss coefficients along with the velocity of the fluid in the section, found by using the continuity equation, the known fluid density, and assuming incompressible subsonic conditions (speeds below Mach 0.3), can be used to calculate the average pressure loss across the section, see the equation. The total pressure loss is calculated by adding up all of the individual section pressure losses.

Pressure Loss Equation Using a Loss Coefficient

This equation allows us to quantify the pressure drop Δp that occurs within a specific section of the wind tunnel circuit. It takes into account the energy lost due to factors like friction in the walls, bends, expansions, and other obstructions.

$$\Delta p = K\frac{1}{2}\rho V^2$$

Where :

Δp *= Pressure loss*

ρ= Fluid density

K= Loss Coefficient

V= Average velocity of the fluid

Calculating pressure losses for each section and summing them up provides the total pressure drop across the entire wind tunnel circuit.

Dimensional Analysis

Wind tunnel testing relies on the concept of flow similarity, which allows us to study the behavior of objects at full scale by testing scaled-down models. This approach is crucial because testing full-scale objects can be expensive and impractical.

Dimensional Analysis of the main fluid mechanics equations of the Navier-Stokes Equation and the Energy Equation leads to four main dimensionless coefficients used to maintain flow similarity; Froude number, Reynolds number, Mach number, and Prandtl number. These numbers help us achieve flow similarity.

Prandtl Number

This number essentially quantifies the relative importance of momentum diffusion (viscous effects) versus thermal diffusion (heat transfer) within a fluid.

$$P_r = \frac{\mu C_p}{k}$$

Where :

P_r= Prandtl number

μ= Fluid viscosity

C_p=Specific heat at Constant Pressure

K= Thermal Conductivity

Mach number

This number compares the velocity of an object or fluid to the speed of sound in the medium. It provides a measure of compressibility effects.

At low Mach numbers (M<0.3), air behaves as an incompressible fluid, meaning its density remains relatively constant. This allows for simpler calculations in low-speed wind tunnels. However, as Mach number increases, air becomes compressible, and its density changes with velocity. This necessitates more complex analysis for high-speed wind tunnels.

$$M = \frac{v}{v_s}$$

Where :

M= Mach number

v= velocity of Object or Fluid

v_s*= Velocity of sound in a Specified medium*

Reynolds Number

This number is the most important in wind tunnel testing. It relates inertial forces to viscous forces within a fluid. The Reynolds number determines wether the flow is laminar (smooth) or turbulent (chaotic and unpredictable). Maintaining similar Reynolds numbers between the model and full-scale object ensures that the flow characteristics are comparable, leading to accurate results.

$$Re = \frac{\rho v l}{\mu}$$

Where :

ρ*= Fluid density*

μ *= Fluid viscosity*

v= Velocity of the fluid

l= Characteristic length

I.6. Applications of wind tunnels

Wind tunnels are essential tools for many industries. They are widely used in a variety of fields to study and visualize the effects of wind on different structures and objects. Here are some of the primary industries that make use of wind tunnels:

I.6.1. Aerospace and Defense

Wind tunnels play a significant role in the design and testing of aircraft, rockets, and satellites. They help analyze the aerodynamic properties like lift, drag, stability, insuring these vehicles navigate the skies efficiently and safely.

I.6.2. Automotive

Wind tunnels are vital in testing and refining vehicles. By optimizing the way air flows around a car, manufacturers can improve fuel efficiency, performance, and the vehicle's overall stability.

I.6.3. Civil Engineering and Architecture

In these fields, wind tunnels are used to analyze the effects of wind on structures like buildings, bridges, and towers. This helps engineers design structures that can withstand wind loads and extreme weather conditions.

I.6.4. Sports Science

Wind tunnels are a training ground for athletes and their equipment. Cyclists, skiers, and racers often use them to refine their posture and equipment design and to maximuze air resistance and performance.

I.6.5. Renewable Energy

Wind turbines are vital tools for designing wind turbines. By testing their aerodynamics, strength, and efficiency, engineers can create turbines that capture more wind energy and operate more reliably.

I.6.6. Marine Industry

Wind tunnels test the above-water parts of ships and offshore structures to improve their aerodynamics, leading to better stability and efficiency.

I.6.7. Rail Industry

High-speed trains are tested in wind tunnels to optimize their design for minimal air resistance, allowing them to handle crosswinds and ensure comfort during travel.

I.6.8. Environmental Science

Wind tunnels are used in environmental studies to simulate and study the dispersion of pollutants in the atmosphere, understand wind patterns, and study wind erosion and deposition processes. [11]

Furthermore, wind tunnel tests encompass various investigations, including :

- Examining model shape effects on aerodynamic characteristics.
- Testing of gas turbines, compressors, propellers, fans, etc.
- Physical testing is concerned with the flow of air under different conditions. Studies of the boundary layer and supersonic flow, etc.
- Methodological research involving wind tunnels as physical instruments, the development of test methods, and the processing of derived data. [12]

Conclusion

In conclusion, wind tunnels serve as essential tools for various scientific and engineering fields. Their ability to simulate airflow and measure airflow characteristics allows researchers to optimize designs and ensure stability across numerous applications. This chapter has established the significance of wind tunnels in this project's research.

Chapter II

Catalytic converters

Introduction

Pollutants emitted from vehicle exhaust have destructive effects on air quality, the environment, and human health, leading to the implementation of strict emission regulations. Various technologies, including engine design upgrades, fuel pre-treatment, alternative fuels, exhaust treatment, and combustion process optimization, are being developed to reduce emissions. Among these, catalytic converters are considered the most effective for controlling hydrocarbon (HC), carbon monoxide (CO), and nitrogen oxide (Nox) emissions from petrol-driven vehicles (gasoline), while particulate filters and oxidation catalysts are preferred for controlling particulate emissions from diesel vehicles. They are now a mandatory component in all vehicles. Thus, catalytic converters are one of the most important advancements in automotive history.

This chapter delves into the inner workings of catalytic converters, exploring their role in reducing harmful pollutants and ensuring cleaner air.

II.1. Catalytic converters

A catalytic converter is an emissions control device. It is a vital part of a vehicle emissions control system. The pollutant gas components are converted into less toxic pollutants by the catalytic action of the catalyst within the converter. The outlet air is eventually released into the atmosphere. Catalytic action in general is the action of certain materials to provoke with their presence in chemical reactions, without themselves being modified by this reaction. Noble metals (platinum and palladium) play the role of these catalysts.

Although catalytic converters are most commonly applied to exhaust systems in automobiles, they are also used on electrical generators, mining equipment, trucks, buses, locomotives, and motorcycles.

II.2. Dangers of polluants

The main emissions of a car engine are :

Nitrogen gas (N_2): Air is 78% nitrogen gas, and most of this passes right through the car engine.

Carbon dioxide (CO_2): A product of combustion, CO_2 forms when carbon in fuel bonds with oxygen from the air.

Water vapor (H_2O): Another product of combustion. The hydrogen in the fuel bonds with the oxygen in the air.

These emissions are generally harmless, although carbon dioxide contributes to global warming. [14]

However, the combustion process is never perfect, producing smaller amounts of more harmful pollutants. Without catalytic converters, that convert nitrogen oxides, carbon monoxide, and hydrocarbons into less harmful chemicals, air quality, particularly in large cities, would become a serious health hazard. [13]

Catalytic converters address these three main concerns: :

Nitrogen oxides (NOx) are compounds of the same family as nitrogen dioxide, nitric acid, nitrous oxide, nitrates, and nitric oxide. NO and NO_2, together are called NOx. Released Nox reacts with organic compounds and sunlight, creating smog. This pollutant has adverse effects on children's lungs. Additionally, NOx interacting with sulfur dioxide produces acid rain, which corrodes cars and has a damaging effect on our environment and our health. Furthermore, NOx can bind with ozone leading to create biological mutations (such as smog) and reducing the transmission of light. It also irritates human mucus membranes.

Carbon monoxide (CO) is a harmful variant of a naturally occurring gas, CO2. Odorless and colorless, CO does not have useful functions in everyday processes. However, it significantly affects oxygen delivery to the body’s organs and tissues, potentially causing death through CO poisoning.

Hydrocarbons (HC) Produced from incomplete combustion of organic fuels. Inhaling HC from gasoline, household cleaners, propellants, kerosene, and other fuels can be fatal, especially to children. Further complications include central nervous system impairments and cardiovascular problems.

II.3. How they work

Catalytic converters work by catalyzing chemical reactions that convert harmful pollutants in the exhaust gases into less harmful substances.

When exhaust gases pass through a heated catalytic converter, two catalytic events (chemical reactions) take place: a reduction catalyst and an oxidation catalyst (see Figure7).

Reduction Catalyst: The first stage, utilizing platinium and rhodium, processes nitrogen oxides (NOx). When an NOx molecule encounters the catalyst, it is broken down. The nitrogen atom is separated and held by the catalyst, while the oxygen is released as O_2. The captured nitrogen atoms then combine with each other, forming harmless N_2 gas that is trapped within the converter.

Oxidation Catalyst: The second stage employs platinum and palladium to address unburned hydrocarbons and carbon monoxide. These pollutants are essentially oxidized by reacting with the remaining oxygen in the exhaust. This reaction, facilitated by the catalyst, transforms CO and hydrocarbons into less harmful CO_2. [15]

Catalytic converter removes harmful byproducts from the exhaust while also improving car efficiency by ensuring complete fuel combustion. This helps maintain a healthy balance of oxygen and fuel in the exhaust which is crucial for optimal converter performance.
The honeycomb structure within the converter is coated with platinum, rhodium, and palladium. These precious metals act as catalysts, accelerating the chemical reactions that transform harmful pollutants. [16]

For example:

2NO => N2 + O2 or 2NO2 => N2 + 2O2

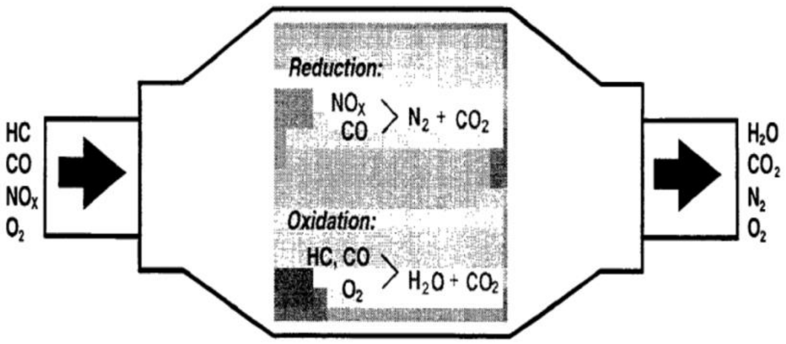

Figure 7: Reactions inside a catalytic converter [15]

For example:

$2CO + O_2 \Rightarrow 2CO_2$

The efficiency of the catalytic converter depends on maintaining the right balance of oxygen and fuel in the exhaust gas. Too much oxygen favors oxidation reactions, while too little oxygen favors reduction reactions.

II.4. Types of catalytic converters

Two-Way Catalytic Converter

Two way catalytic converters, also called oxidation catalysts, are named for their ability to target two main pollutants in exhaust gases: hydrocarbons (HC) and carbon monoxide (CO). These pollutants arise from incomplete fuel combustion, where some fuel (HC) remains unburned and CO forms due to a lack of sufficient oxygen.

Oxidation converter components are normally canvassed in platinum. In a two-way catalytic converter mainly two tasks simultaneously occur. One is oxidation of carbon monoxide to carbon dioxide. Another one is the oxidation of unburnt and partially burnt hydrocarbons to carbon dioxide and water. These two types of oxidation reactions, it is also known as oxidation-type catalytic converters.

Conversion Reactions in Two-Way Catalytic Converter

$C_xH_{4x} + 2xO_2 \rightarrow xCO_2 + 2xH_2O$ (conversion of hydrocarbons)

$2xCO + O_2 \rightarrow 2xCO_2$ (conversion of carbon mono-oxides)

Three-way Catalytic Converter

Unlike two-way converters, three-way catalytic converters, also known as reduction catalysts, address a boarder range of pollutants in exhaust gases. They can process hydrocarbons (HC) and carbon monoxide (CO), like oxidation converters, but also significantly reduce nitrogen oxide (Nox) emissions. This is particularly important because Nox forms in the engine’s combustion chamber at extremely high temperatures. [17]

A three-way catalytic converter has three simultaneous functions:

1. Reduction of nitrogen oxides into elemental nitrogen and oxygen: (Decomposition of oxides of nitrogen)

   $NO_x \rightarrow N_x + O_x NO_x \rightarrow N_x + O_x$

2. Oxidation of carbon monoxide to carbon dioxide: (conversion of carbon mono-oxides)

$CO+O2 \rightarrow CO2CO+O2 \rightarrow CO2$

3. Oxidation of hydrocarbons into carbon dioxide and water: (conversion of hydrocarbons)

   $CxH4x+2xO2 \rightarrow xCO2+2xH2OCxH4x+2xO2 \rightarrow xCO2+2xH2O$

II.5. Composition of catalytic converters

Catalytic converters, indispensable components within modern vehicle exhaust systems, are meticulously engineered to reduce harmful emissions effectively. They comprise a complex interplay of various components, each contributing significantly to the overall efficiency of the system. Understanding the detailed composition of catalytic converters is crucial for optimizing their performance and advancing emission control technology. [18]

II.5.1. Core or Substrate

At the core of catalytic converters lies the substrate, a ceramic or metallic honeycomb structure. This design maximizes surface area, allowing for optimal interaction between exhaust gases and the catalysts. [19]

II.5.2. The Wash Coat

The wash coat is a thin layer of silica and alumina applied to the substrate. It plays a critical role in boosting catalytic performance. It helps increase the available surface area for the catalysts to perform on. This rough and irregular surface creates numerous active sites where crucial chemical reactions take place, optimizing the conversion efficiency of harmful pollutants.

II.5.3. The Catalyst

The catalyst consists of precious metals such as platinum, palladium, or rhodium. These noble metals serve as active agents, facilitating the conversion of harmful pollutants into less harmful substances through chemical reactions.

II.5.4. Metal Casing

The metal casing provides vital structural support and thermal management for the catalytic converter. It is designed to resist the harsh environment it operates in, including vibrations and extreme temperatures. Thin-walled casings are preferred to ensure efficient heat transfer, preventing the converter from overheating and compromising its effectiveness.

II.6. Efficiency of catalytic converters

The efficiency of catalytic converters plays a vital role in reducing harmful emissions from vehicles. By studying this efficiency, we can continuously improve the design and performance of these essential components.

The main three ways of evaluating the catalytic efficiency are as follows:

Monitoring Nox and CO levels:

A common method involves measuring the levels of nitrogen oxides (NOx) and carbon monoxide (CO) in the exhaust gas. Sensors are installed at two key points:

Before the catalytic converter, this sensor measures the initial concentration of Nox and CO in the exhaust.

After the converter, this sensor measures the remaining Nox and CO levels.

Using oxygen sensors:

Another technique relies on oxygen sensors strategically positioned before and after the converter. These sensors monitor the oxygen content in the exhaust gas.

Efficient catalytic conversion processes consume oxygen while transforming pollutants. Comparing pre and post converter oxygen levels can indicate the effectiveness of the converter.

Using Temperature Sensors:

The third method involves measuring the temperature of the exhaust pipe before and after the converter. This approach assumes that an efficiently functioning catalytic converter generates more heat.

II.7. Conditions in Catalytic converters: Temperature and Pressure inside a catalytic converter

Table 1 provides data obtained to determine pressure and temperature inside a catalytic converter.

It can be seen that the heat treatments at 400 and 600 ºC are highly effective in enhancing the activity and stability of the composites. [20]

The temperature inside a catalytic converter needs to reach a moderately high level for optimal efficiency, typically around 400-600°C. The pressure inside the converter is influenced by factors such as flow dynamics and the design of the exhaust system .

Table 1: Temperature and pressure values from different sources

Source	Temperature	Pressure
Article: Catalytic Converter Simulation for Pressure and Velocity Measurement	400 to 600 degrees Celsius	Inlet pressure = 7.37 bar Inside = between 6.9 and 2.3 bar Outlet = 0.45 to 0.9 bar
Article: Understanding Flow through catalytic converters	Inlet = 177 degrees Celsius Near boundary layer = 110 degrees Celsius	Inlet pressure = 3250 Pa Inside = from 3000 to 250 Pa Outlet pressure = 0 Pa
Article: Study Influence of Core Structure on Catalytic Converter Performance Using CFD	-	Inlet pressure = 319,22Pa Outlet pressure = 0 Pa

$$\frac{dT_{cat,out}}{dt} = -\frac{4.\dot{m}_{exh}.c_{p,exh}}{L.(1-\varepsilon).\rho_s c_{p,s}\pi D_s^2}(T_{cat,out} - T_{cat,in})$$

Where :

T= the substrate's temperature

ρ_s *= The density of the substrate*

$c_{p,s}$ *= Specific heat capacity of the substrate*

D_s *= Diameter of the substrate*

L= Catalyst length

ε *=The void fraction*

Conclusion

Catalytic converters play a vital role in minimizing the environmental impact of vehicles. They function by utilizing precious metals to convert harmful pollutants into less toxic substances. This conversion process necessitates a specific operating environment, with optimal temperatures ranging from 400 to 600^{o}C.

Chapter III
Mesh

Introduction

Mesh generation is a crucial step in CFD simulation using ANSYS Fluent. It involves creating a computational mesh that discretizes the domain into smaller elements. Selecting an appropriate meshing method is essential for capturing the complexities of the geometry and flow phenomena.

This chapter tackles mesh generation, exploring different meshing methods and analyzing their impact on accuracy. A case study will be performed to demonstrate mesh generation in action.

III.1. Numerical methods for CFD Simulations : FVM and FEM

In the realm of Computational Fluid Dynamics (CFD), two primary numerical methods dominate the Finite Volume Method (FVM) and the Finite Element Method (FEM). Both techniques are powerful tools for solving the governing equations of fluid flow, heat transfer, and other phenomena. However, they differ in their underlying concepts, strengths, adn suitability for specific applications.

Finite Volume Method (FVM)

FVM subdivides the simulation domain into a network of small control volumes (cells). These control volumes can be of various shapes (tetrahedra, hexahedra, etc.) depending on the complexity of the geometry.

The governing equations of fluid flow (Navier-Stokes equations) are then integrated over each control volume. This integration process enforces the conservation of mass, momentum, and energy within each volume.

FVM can effectively handle complex geometries and boundary conditions by adapting the control volume shapes to fit the domain. It is also well-suited for solving Navier-Stokes equations, making it ideal for simulating fluid flow phenomena.

Finite Element Method (FEM)

The finite element method offers a different approach to solving CFD problems. FEM divides the domain into finite elements. It then uses interpolation functions to approximate the solution variables within each element.

FEM excels in handling complex geometries due to its flexible element shapes. However, FEM can be computationally more expensive compared to FVM if applied to CFD problems.

III.2. Mesh generation methods

Mesh generation is a critical first step in any CFD simulation using ANSYS Fluent. It involves creating a computational mesh, essentially a grid that discretizes the simulation domain into smaller elements (cells). Selecting an appropriate mesh generation method is crucial for capturing the complex geometries and flow phenomena.

Types of mesh generation methods

Structured meshing: This method creates a grid with a regular, ordered pattern of cells, typically cubes or hexahedra. It is efficient for simple geometries due to the predictable arrangement. The regular structure of elements allows for accurate calculations and minimizes numerical errors. However, this type of mesh can be challenging to apply to complex geometries with intricate features or curved surfaces.

Unstructured meshing: This method uses cells of various shapes, such as tetrahedra, hexahedra (used for simpler regions), and pyramids, offering greater flexibility in handling intricate and irregular geometries. This type of mesh can conform to complex shapes, making them ideal for capturing detailed features. However, it can increase computational costs due to the irregular nature of the meshes (see Figure 8).

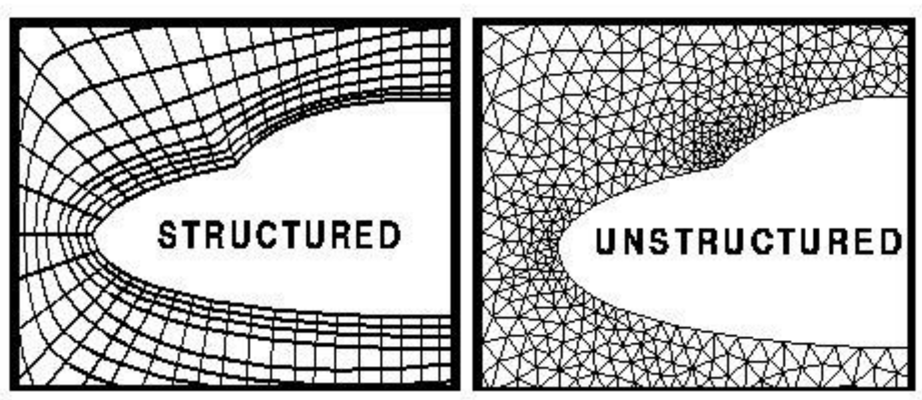

Figure 8: Structured and unstructured mesh [22]

Hybrid meshing: This method combines structured and unstructured grids, exploiting the advantages of both approaches within the same simulation. This helps to obtain optimized efficiency and accuracy; structured meshes can be used in regions with simpler geometry, while unstructured meshes handle more complex areas. This optimizes the balance between computational efficiency and accuracy. [23]

III.3. Mesh quality and criteria

Mesh quality is the base of a reliable CFD simulation in ANSYS Fluent. It directly impacts the accuracy, convergence, and stability of the numerical solution obtained.

A high-quality mesh allows for an accurate representation of the geometry and facilitates the numerical calculations, leading to more reliable results and helping with capturing the flow phenomena.

Convergence refers to the solution reaching a stable state with further refinement having minimal impact. A high-quality mesh promotes smoother convergence of the solution during the simulation process.

Poor mesh quality can introduce numerical errors and instabilities, potentially leading to unrealistic or non-converging simulations.

To ensure high quality mesh, several criteria are used to evaluate the geometric attributes of the computational cells.

Aspect Ratio: Aspect is defined by the ratio of the longest edge to the shortest edge of a cell. Ideally, the aspect ratio should be close to 1. Deviation from this value indicates distortion in the element shape. Some deviation is tolerable, but excessively high aspect ratios can affect the solution’s accuracy.

Skewness: Skewness is the deviation of a cell from orthogonality. Ideally, elements should have all sides meeting at right angles, ensuring a well-defined geometric structure. High skewness occurs when element sides become significantly non-orthogonal, leading to distorted shapes. A value of 0 indicates a perfect shape, with lower values generally considered better. A skewness below 0.3 is considered acceptable for most CFD simulations. [21]

Orthogonality: Orthogonality shows how perpendicular the cell faces are relative to each other. Ideally, cell faces are perfectly orthogonal. Higher orthogonality values are preferable as they minimize discretization errors associated with non-orthogonal faces. With two neighboring elements in the grid, moving from one element to the other, when the line connecting the center of each of these elements is orthogonal to the interface, that indicates a good-quality mesh. Thus, in an orthogonal mesh, the line connecting the centers of adjacent elements is perpendicular to their shared interface. Otherwise, the mesh quality is poor. Figure 9 illustrates an orthogonal and a non-orthogonal mesh. [26]

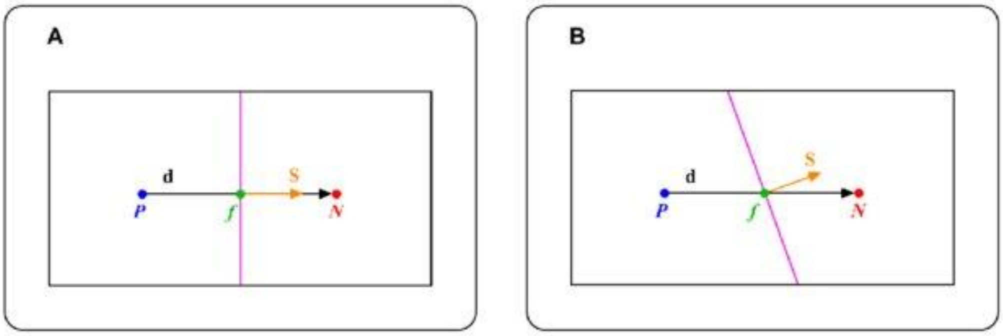

Figure 9: Mesh orthogonality A(orthogonal), B (non-orthogonal) [24]

Smoothness (grid transition) : Smoothness, as shown in figure 10, ensures gradual changes in cell size throughout the mesh. Abrupt variations in cell size can introduce numerical instabilities and affect solution accuracy. [21]

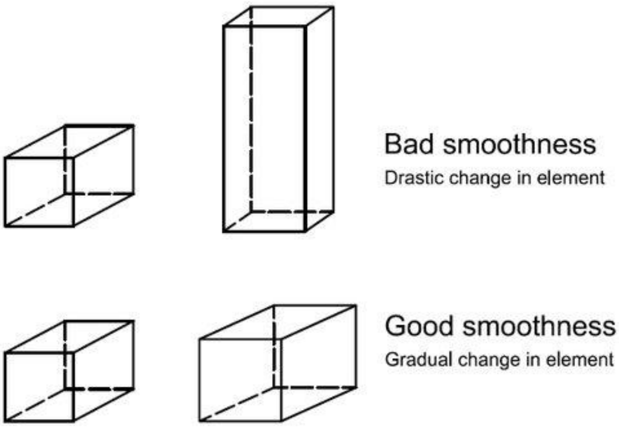

Figure 10: Mesh smoothness [25]

III.4. Mesh density and refinement

Mesh density and refinement are fundamental aspects of achieving reliable and efficient CFD simulations in ANSYS Fluent.

Mesh density :

Mesh density refers to the number of computational cells (elements) discretizing the simulation domain. A higher mesh density translates to a finer mesh with more cells.

Generally, a mesh density leads to more accurate results, this is because it allows for better resolution of gradients, or sharp changes, in flow properties, such as velocity or temperature. However, excessively high mesh density can significantly increase computational cost. [27]

Mesh refinement :

Mesh refinement is a technique to strategically increase the mesh density in specific regions of the domain where high gradients or complex flow patterns are expected. These regions typically include walls (boundary layers with significant velocity and temperature gradients), and obstacles (regions with flow separation or recirculation behind obstacles). [21]

III.5. Mesh Sensitivity Analysis

Mesh sensitivity analysis is a critical step in ensuring the reliability of the simulations. It guarantees that the numerical solution is independent of the mesh resolution used.

Importance of Mesh Sensitivity Analysis :

A finer mesh generally leads to more accurate results, but it also increases computational time and resource requirements. Mesh sensitivity analysis helps find a balance between these two factors. [28]

By demonstrating mesh independence, our numerical model used for the simulation is validated. This strengthens the credibility of the results and optimization of catalytic converter devices. [21]

Methodology :

The process involves systematically refining the mesh and observing the impact on key output parameters relevant to the performance.

1. Generating meshes: Creation of a series of meshes while increasing element sizes (coarser to finer)
2. Solving the CFD model for each mesh: It is important to run the CFD simulation for each mesh with the same settings

3. Monitoring key output parameters: Tracking essential parameters relevant to the problem.
4. Convergence analysis: Comparison of the results from each mesh. If the key parameters show minimal change with further mesh refinement, the current mesh can be considered sufficiently fine.
5. Refinement or Alternative Strategies: If significant variations persist, further mesh refinement or exploring different meshing strategies might be necessary. This could involve changing element types (tetrahedral, hexahedral, etc.) or employing adaptative meshing techniques (region-based refinement, etc.).

III.6. Mesh of a simplified geometry

Firstly, a pipe’s geometry was created using the Geometry Design Modeler

Using the component system « Fluent with Fluent Meshing » in the workbench, different types of meshing were tried out, notably tetrahedral, hex-core, polyhedra, and poly-hexcore.

For the sensitivity analysis, different parameters were tested out within « Create Volume Mesh »; Max Cell Length, Growth Rate, and Buffer layers were the most important ones to work with. For further detailed analysis, adjustments were made in « Add Boundary Layer », including growth rate, number of layers, and transition ratio.

Improving the mesh resolution near the boundary layer is very crucial it helps capture flow phenomena more accurately, such as the velocity gradients which are very high in that region.

After that, the simulation results were visualized using ANSYS Fluent tools. Static pressure contours on pipe walls and velocity contours in mid-planes provided insights into flow behavior. The comparison between the different mesh types and parameter configurations was made to determine the optimal settings for convergence and computational efficiency.

Using the following equations, the velocities that were used in the setup were determined.

$$D_h = \frac{4\,A}{P}$$

Where :

D_h= Hydraulic diameter

A= surface of the cross-section of the duct

P= perimeter of the cross-section of the duct

$$Re = \frac{V.D_h}{\vartheta}$$

Where :

Re= Reynold's number

V= Velocity of the fluid

ϑ= Kinematic viscosity of the fluid

For polyhedra and poly-hexcore types of mesh, the pressure contours and the velocity contours, for respectively five and six different growth rates and max cell lengths, were generated in order to assess the impact of the variation of these parameters on the flow behavior within the computational domain (see table 2 and 3).

The velocity obtained is 3m/s,the diameter of the pipe D=0.05m, and the length of the pipe is L=0.2m

Table 2: Pressure and velocity contours using polyhedral type of mesh

	Pressure contour	Velocity contour
Polyhedra, Growth Rate=1.2, Max Cell length=0.008	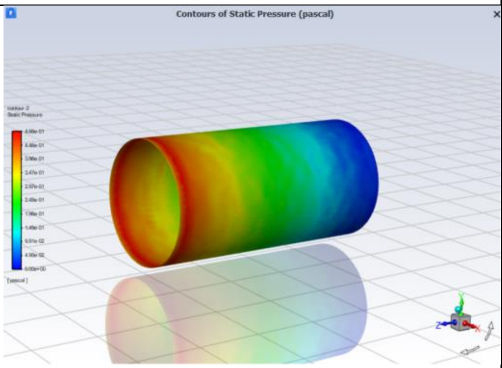	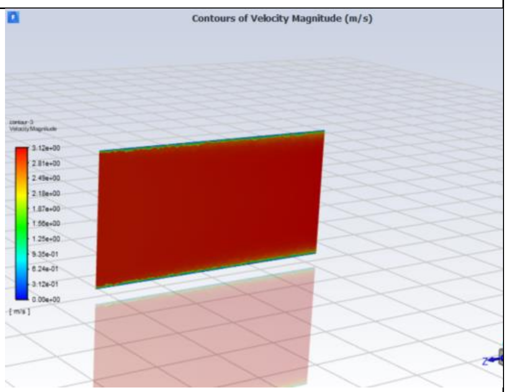
Values	Maximal Pressure =0.496 Pa	Maximal Velocity =3.12 m/s

Polyhedra, Growth Rate=1.1, Max Cell length=0.007	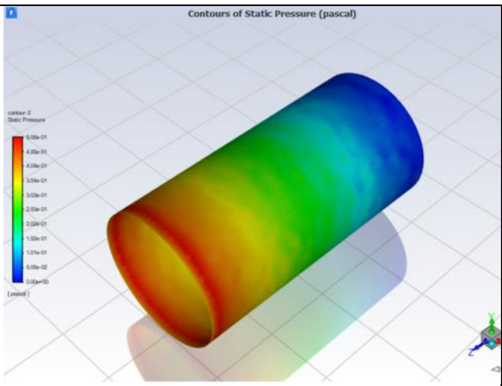	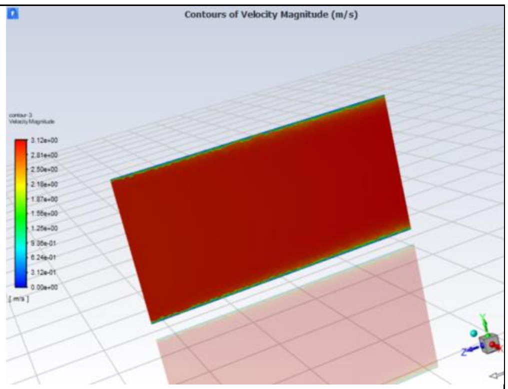
Values	Maximal Pressure =0.505 Pa	Maximal Velocity =3.12 m/s
Polyhedra, Growth Rate=1.08, Max Cell length=0.006	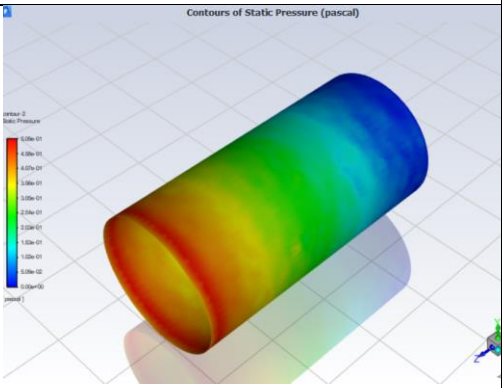	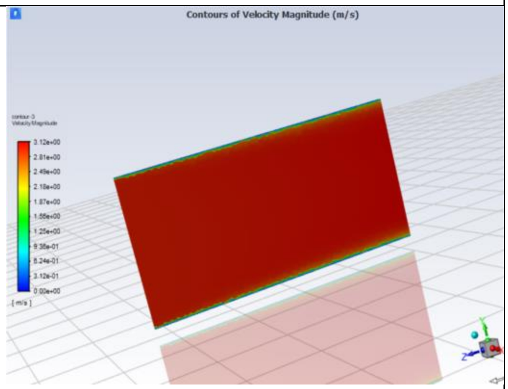
Values	Maximal Pressure =0.509 Pa	Maximal Velocity =3.12 m/s
Polyhedra, Growth Rate=1.06, Max Cell length=0.005	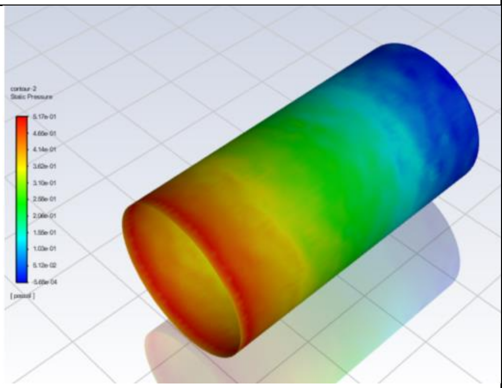	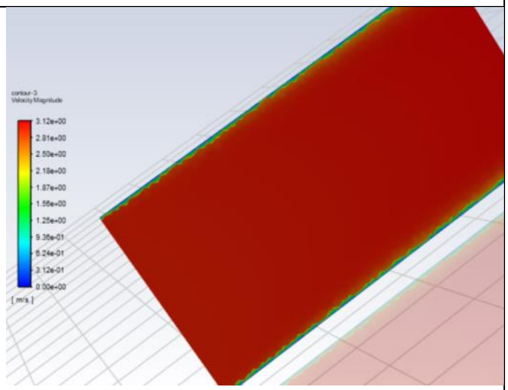
Values	Maximal Pressure =0.517 Pa	Maximal Velocity =3.12 m/s

Polyhedra, Growth Rate=1.05, Max Cell length=0.004	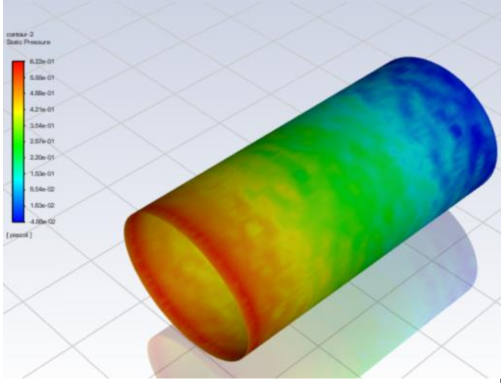	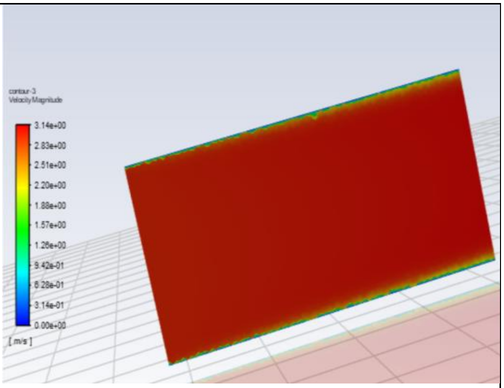
Values	Maximal Pressure =0.622 Pa	Maximal Velocity =3.14 m/s

Interpretation :

As the mesh goes from coarse to fine, the values of the maximum static pressure have increased from 0.496 Pa to 0.622 Pa. The values of maximum velocity magnitude have slightly increased, from 3.12 m/s to 3.14 m/s.

Conclusion

We can conclude that the coarser mesh, with a growth rate of 1.2, and max cell length of 0.008 helped us get as detailed results as with the finer mesh. We are thus allowed to use the coarse mesh for our simulation in order to reduce the computational cost and time while having accurate results.

Table 3: Pressure and velocity contour using poly-hexcore type of mesh

	Pressure contour	Velocity contour
Poly-hexcore, buffer layer=2, max cell length=0.008	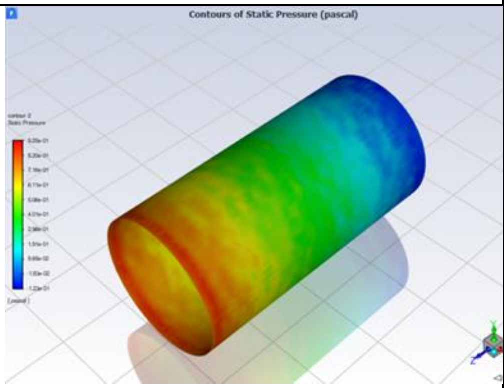	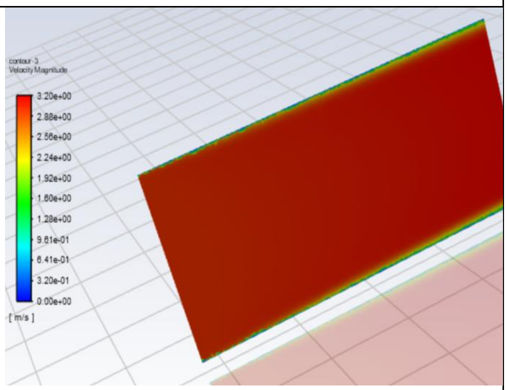
Values	Maximal Pressure =0.926 Pa	Maximal Velocity =3.20 m/s

Poly-hexcore, buffer layer=3, max cell length=0.007	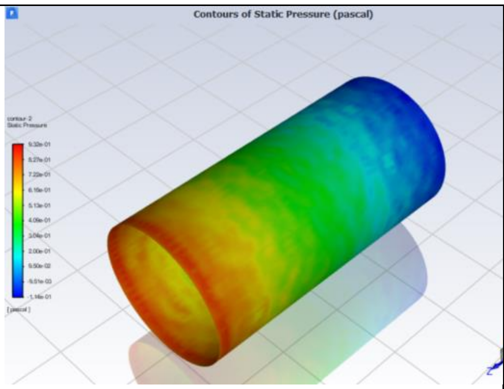	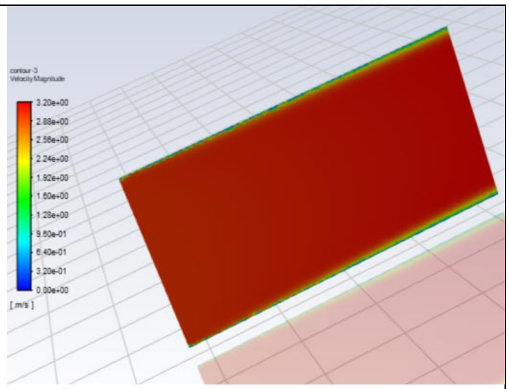
Values	Maximal Pressure =0.932 Pa	Maximal Velocity =3.20 m/s
Poly-hexcore, buffer layer=4, max cell length=0.006	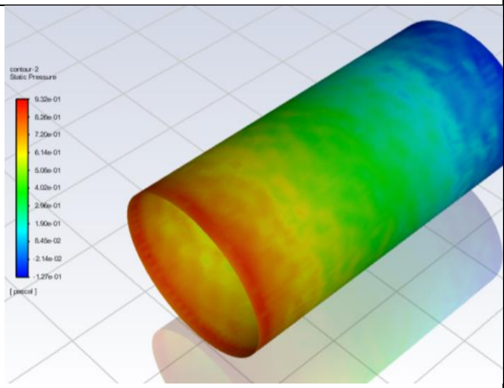	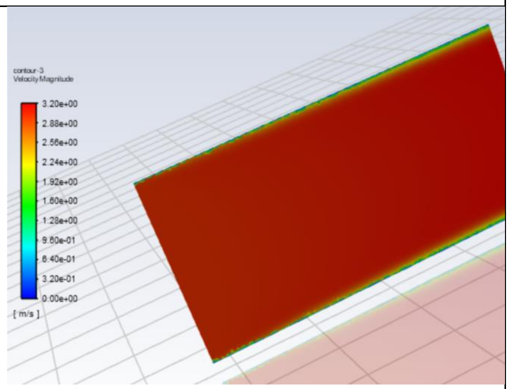
Values	Maximal Pressure =0.932 Pa	Maximal Velocity =3.20 m/s
Poly-hexcore, buffer layer=5, max cell length=0.005	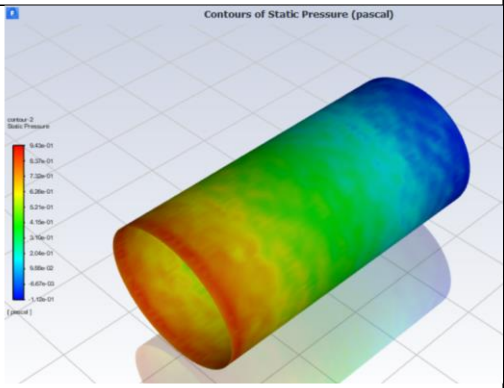	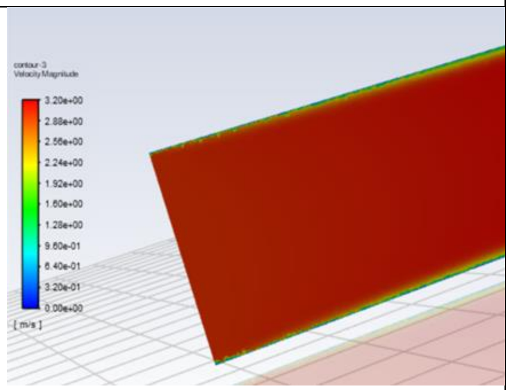
Values	Maximal Pressure =0.943 Pa	Maximal Velocity =3.20 m/s
Poly-hexcore, buffer layer=6, max cell length=0.004	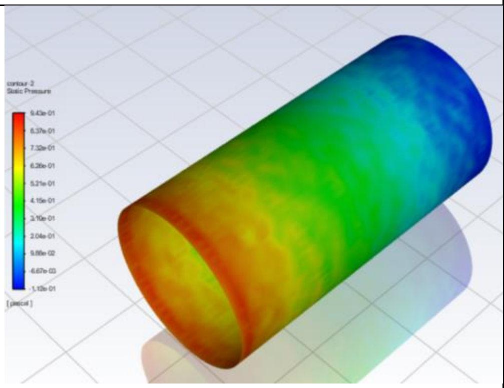	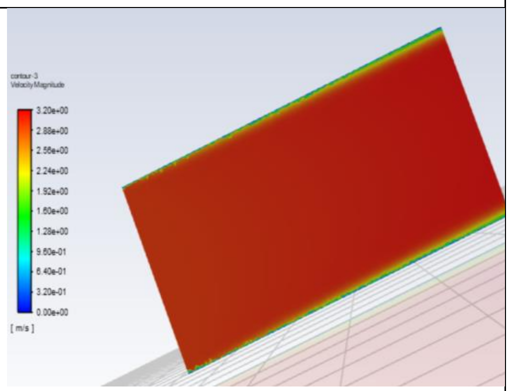
Values	Maximal Pressure =0.943 Pa	Maximal Velocity =3.20 m/s

Poly-hexcore, buffer layer=8, max cell length=0.002	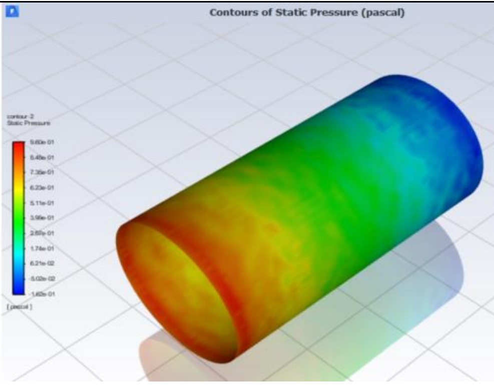	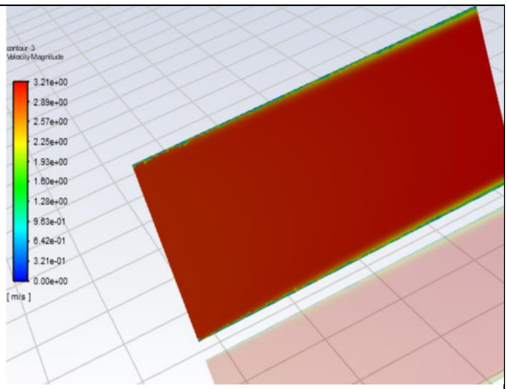
Values	Maximal Pressure =0.960 Pa	Maximal Velocity =3.21 m/s

Interpretation

From coarse to fine, the results have varied from a maximum pressure of 0.926 Pa and a maximum velocity magnitude of 3.20m/s to a maximum pressure of 0.960Pa and a maximum velocity magnitude of 3.21m/s.

Conclusion

The coarse mesh (Poly-hexcore, buffer layer=2, max cell length=0.008) can be used for our simulation in order to reduce the computational cost and time.

Conclusion

This chapter explored mesh generation methods in ANSYS, Fluent, emphasizing their impact on the accuracy and efficiency of CFD simulations. Mesh sensitivity was introduced as a vital step to ensure mesh independence, a crucial aspect of obtaining reliable simulation results. Thie chapter concluded by presenting a case study demonstrating mesh generation using different mesh types and parameter configurations for a simplified geometry.

Chapter IV
Material and methods

Introduction

This chapter describes the main tools and methods that have been used in the design, simulation, and experimental validation of certain device. The software used for creating the 3D models and performing Computational Fluid Dynamics simulations are going to be explored. Additionally, the physical components used are going to be described.

IV.1. Design software

CATIA V5: CATIA V5 is a leading software in the field on Computer-aided Design (CAD). It provides engineers and designers with an extensive range of tools for creating highly detailed and precise 3D models. These models can represent anything from individual components to complex assemblies. In this project, CATIA V5's strength in 3D modeling was exploited to create a total of 36 filter designs. Various filter configurations were explored, including designs with internal tubes for a more focused airflow path, honeycomb structures to promote even distribution, incorporating wire mesh to improve the filter's efficiency.

ANSYS Fluent: ANSYS Fluent is a Computational Fluid Dynamics (CAD) software. Unlike traditional physical testing, CFD software creates virtual environments to analyze how fluids, like air, behave under various conditions.This allows engineers to gain valuable insights into fluid flow patterns, pressure distribution, and other factors without the need for expensive and time-consuming physical prototypes. In this project, the 3D filter models from CATIA V5 were imported into ANSYS Fluent. Additionally, a small scaled wind tunnel design and a model of the fan heater were incorporated, to simulate the airflow. By running these simulations, the airflow patterns within the filters will be analyzed and compared. It will show how each filter design impacts the uniformity of the airflow exiting the filter.

IV.2. Physical components

- **Wind Tunnel:** A small-scale open wind tunnel was used to replicate real-world airflow conditions in a controlled environment.

- **Catalytic Converter:** the catalytic converter used in this project is a small-scale model made of steel, designed to mimic real-world exhaust conditions.
- **Leister Mistral Fan:** Our experiment required precise control over both airflow and temperature. To achieve this, we used the Leister Mistral Fan (see figure 11), specifically Mistral 6 System, which can deliver variable air speeds and temperatures. This fan has a power of 4500 watts and can move up to 400 l/min of air at its highest setting. Additionally, it can heat the air up to 650º, and it operates under high pressure, up to 3.5 kPa.

Figure 11: The fan heater device of university's laboratory

- **Device for uniform flow (filter):**

A total of 36 unique filter models were designed to investigate the impact of filter configuration on achieving uniform airflow before it entered the catalytic converter. Each filter model had a diameter of 59mm and a thickness of 1,5mm. The filter variations explored two primary internal structures: tubes and honeycombs. The tables 4, 5, 6, and 7 illustrate the different designs of the filters designed using the software Catia V5.

Tube-based Filters: Eighteen filter models incorporated internal tubes of varying diameters. These diameters were chosen from a manufacturer's catalog and included 5 mm, 7 mm, and 9 mm. All tubes had a wall thickness of either 0.25 mm (for 5 mm and 7 mm diameters) or 0.3 mm (for 9 mm diameter) as specified by the catalog. The specific arrangement and number of tubes within each filter model were determined using a circle packing algorithm. This algorithm is a computational tool used to efficiently pack circles within a specific container, in our case, it is a diameter of 59 mm. The algorithm aims to maximize the number of circles (tubes) while minimizing any gaps between them.

Honeycomb-based Filters: Other eighteen filter models utilized honeycomb structures as their primary internal element. These honeycombs were also sourced from a manufacturer's catalog and came in three different internal diameters: 7.5 mm, 9.5 mm, and 12.7 mm. All honeycombs had a thickness of 0.2 mm.

Wire mesh: The wire mesh has a spacing of 1.5 mm between individual cylinders and a wire diameter of 0.2 mm.

Table 4: Tube-based filters without wire mesh

	L=10	**L=20**	**L=30**
D=5	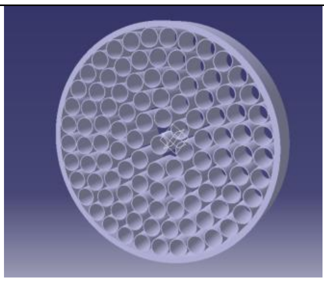	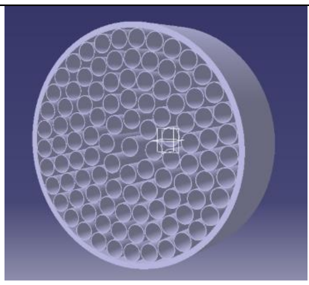	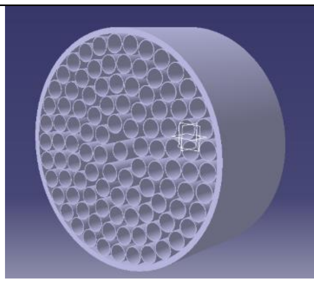
D=7	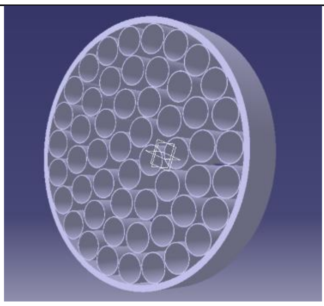	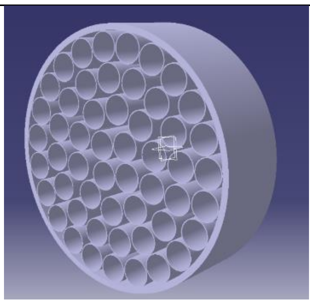	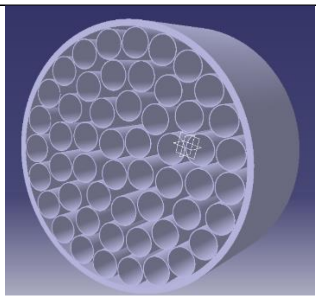
D=9	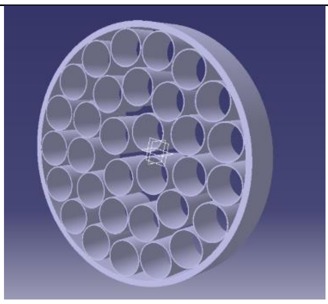	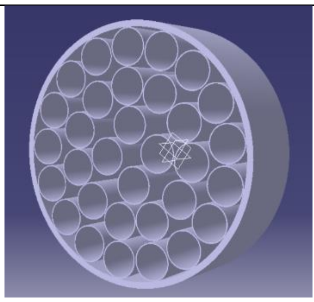	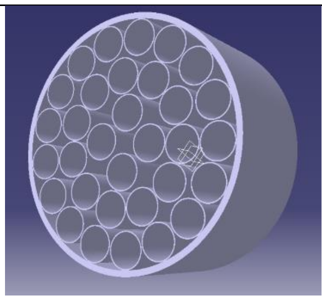

Table 5: Tube-based filters with wire mesh

	L=10	**L=20**	**L=30**
D=5	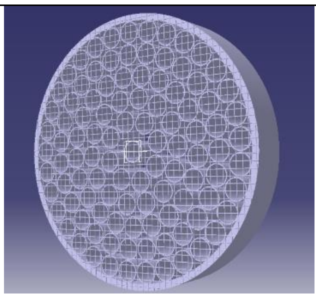	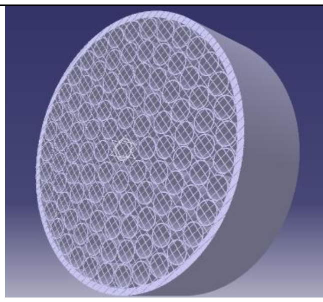	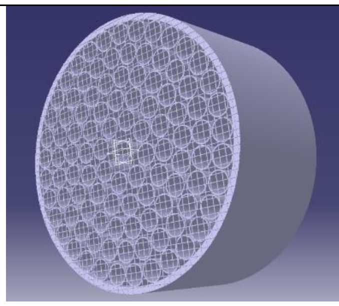
D=7	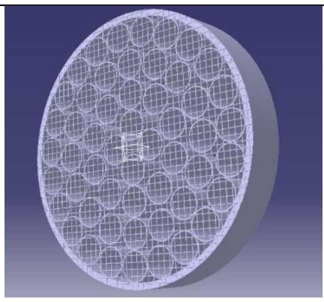	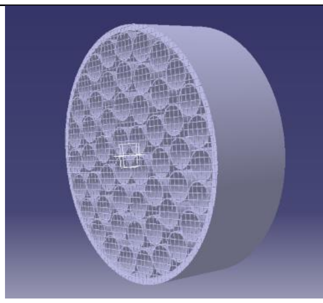	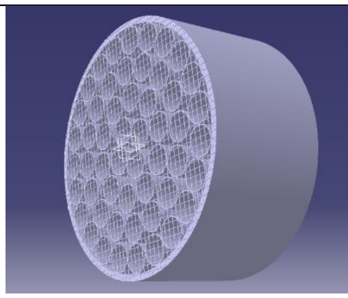
D=9	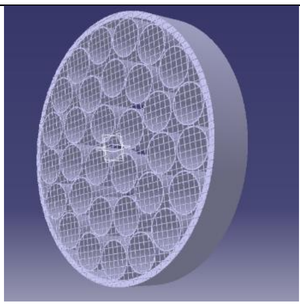	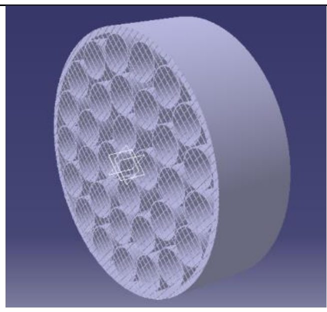	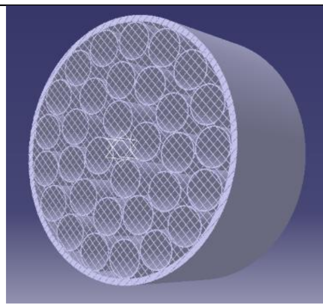

Table 6: Honeycomb-based filters without wire mesh

	L=10	L=20	L=30
D=7,5	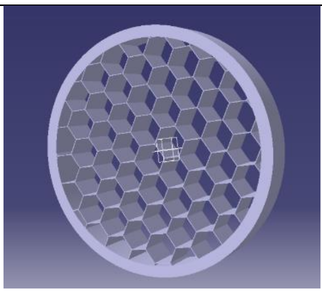	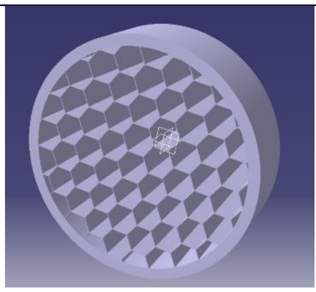	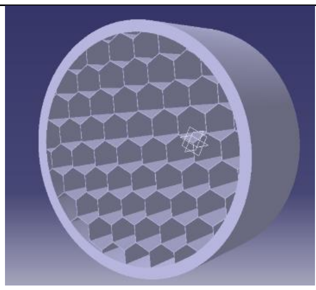
D=9,5	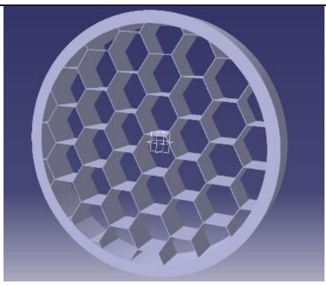	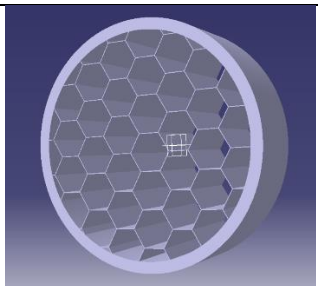	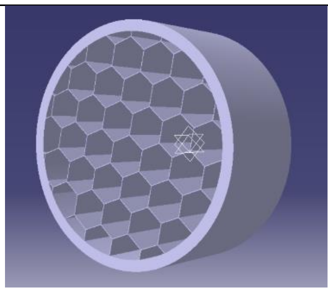
D=12,7	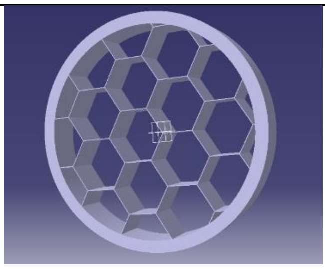	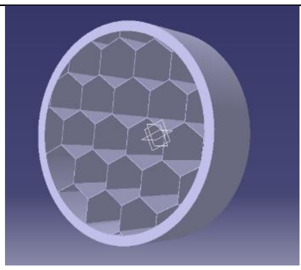	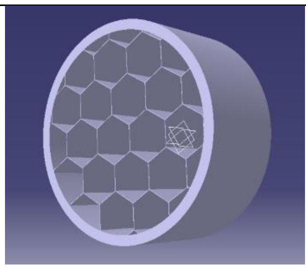

Table 7: Honeycomb-based filters with wire mesh

	L=10	L=20	L=30
D=7,5	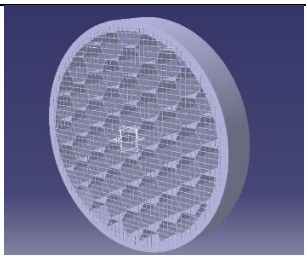	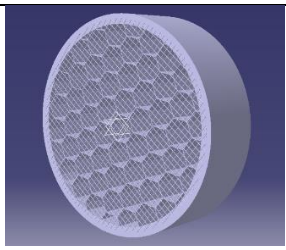	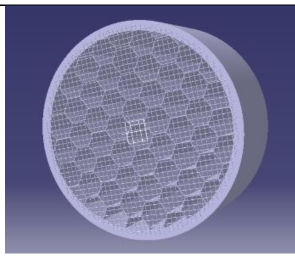
D=9,5	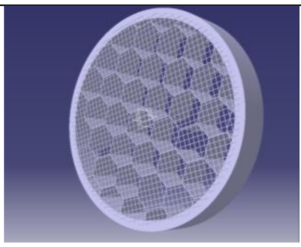	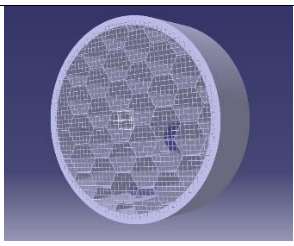	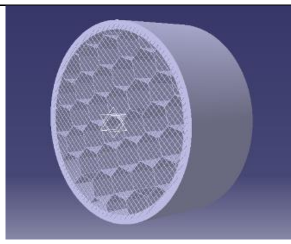
D=12,7	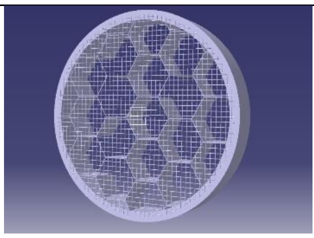	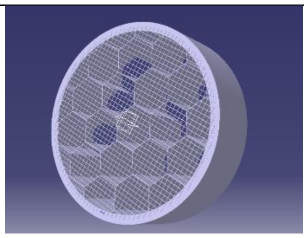	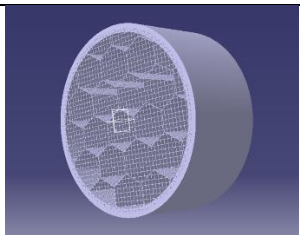

IV.3. Airflow velocity measurements

The laboratory experiments helped us characterize the airflow behavior exiting the fan heater at different power levels. The fan power was varied from 1% to 100% of its capacity. The velocity of the airflow was measured across the outlet diameter at three locations. The center (y=0) and the lateral positions (y=15 and y=-15). These measurements were captured using a hot wire anemometer. The resulting data is presented as an Excel graph, illustrated in Figure 12, with multiple colored curves, each curve representing the velocity profile at a specific fan power setting. Additionally, arrows were incorporated into the graph to illustrate the radial nature of the airflow exiting the fan heater.

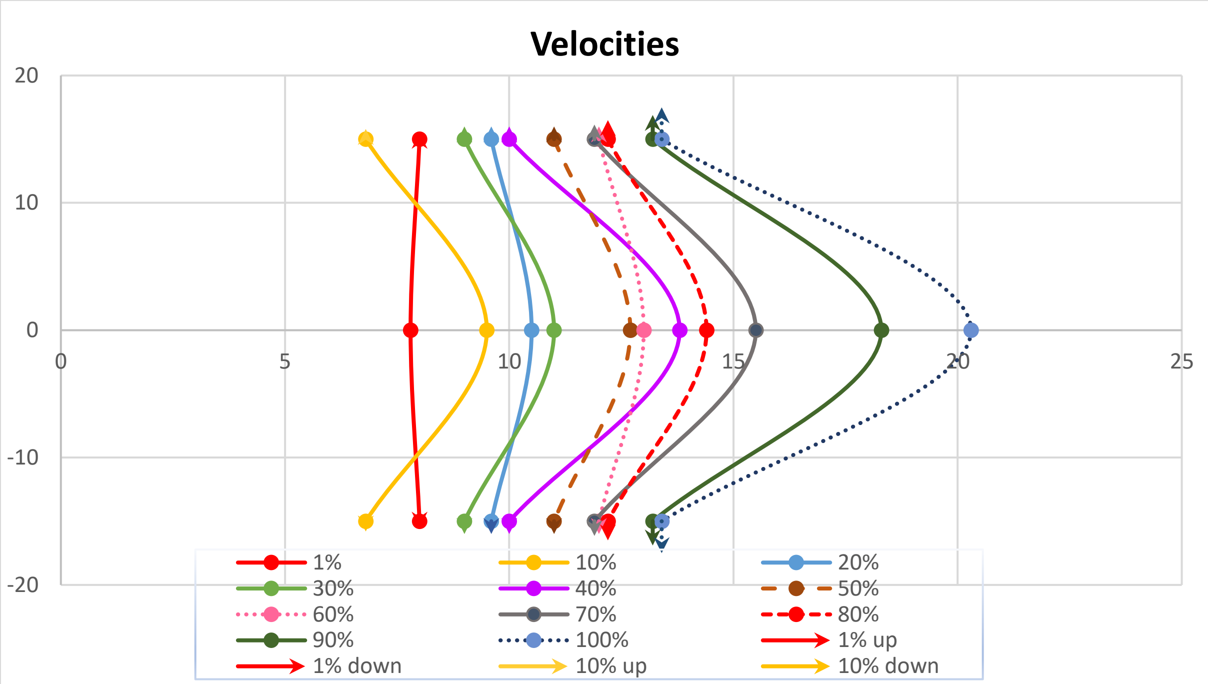

Figure 12: Velocity at the outlet of the fan heater using different power

IV.4. Temperature measurements

Similar to the airflow velocity measurements, the laboratory experiments also characterized the temperature distribution at the outlet of the fan heater across different power levels (1% to 100%). The temperature data is presented as an Excel graph with a straight line for each power level (see figure 13).

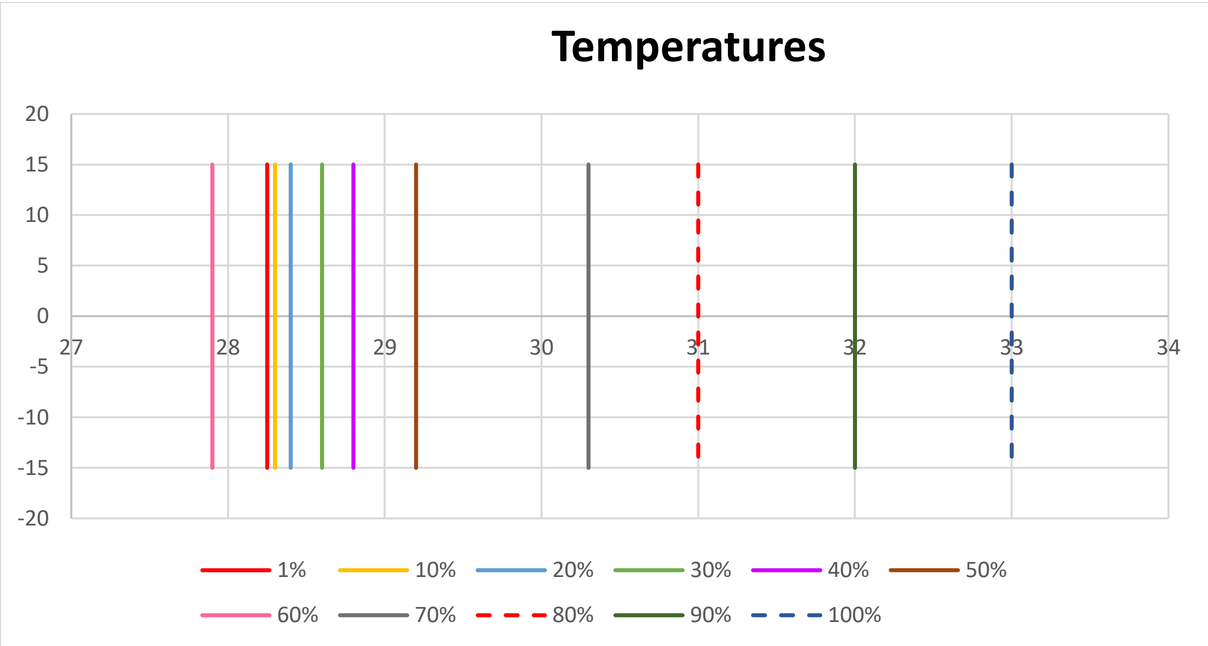

Figure 13: Temperature at the outlet of the fan heater using different power

Conclusion :

This chapter provided a comprehensive overview of the software tools, physical components, and filter variations utilized throughout the project. By utilizing advanced design software with CFD simulations, we aimed to gain valuable insights into the impact of filter design on achieving a uniform airflow exiting the device, ultimately influencing the performance of the catalytic converter.

Chapter V
Results

Introduction

This chapter investigates the flow behavior within a fan heater using CFD simulation. It aims to understand the airflow and characteristics for optimizing its performance and efficiency.

This chapter is structured as follows, boundary conditions will be described, as well as the geometry of the fan heater model used in the simulation. Next, the meshing and setup processes will be described. Finally, the key findings obtained from the simulation will be presented, focusing on the analysis of the flow's distribution and characteristics. A discussion of the results will highlight the significance of the simulation of understanding the fan heater's performance and potential areas for improvement.

V.1. Description of the boundary conditions

Figure 14 illustrates the boundary conditions implemented within the CFD simulation of the fan heater. These conditions define the operating environment and airflow characteristics within the model.

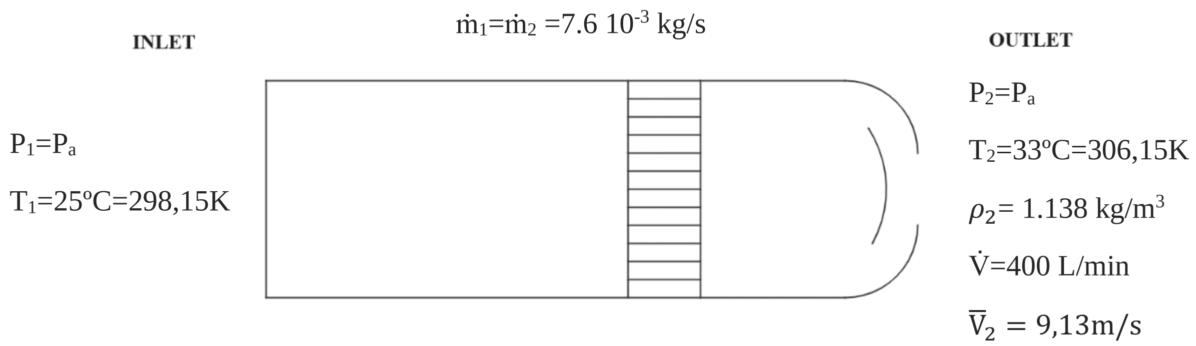

Figure 14: Boundary conditions of the Fan Heater

A critical parameter is the mass flow rate of air entering the domain. The air volume was obtained from the manufacturer's catalog specifications. It is denoted as $\dot{V}_2$ and equals 400 liters per minute which translates to 6,66. 10^{-3} cubic meters per second. This helps us obtain the mass flow, which should be an equal value both at the inlet and the outlet.

$$\rho_2 = \frac{P_2}{R.T_2} = \frac{10^5}{287\,.\,306{,}15} = 1{,}138\; kg/m^3$$

$\dot{V}_2$= 400 L / min = 6,66. 10^{-3} m^3/s (max air volume, given by the manufacturer catalog)

$\dot{m}_2 = \dot{m}_1 = \rho_2 \dot{V} = 1{,}138 . 6{,}66 . 10^{-3} = 7{,}579\ kg/s$

$$A_2 = \pi . r^2 = \frac{\pi . D^2}{4} = \frac{\pi . 0{,}0305}{4} = 0{,}7302 . 10^{-3} m^2$$

$$\bar{V}_2 = \frac{\dot{V}_2}{A_2} = \frac{6{,}66 . 10^{-3}}{0{,}7302 . 10^{-3}} = 9{,}13\ m/s$$

$\bar{V}_2$ represents the average speed at which air exits the domain.

The number of Reynolds is presented by the following equation :

$$Re = \frac{\rho V D}{\mu}$$

At 33ºC, the dynamic viscosity of the air is μ =1,874.10^{-5} kg.m^{-1}.s^{-1}

$$Re = \frac{1{,}138 . 9{,}13 . 0{,}0305}{1{,}874 . 10^{-5}} = 16909.988$$

The calculated Reynolds number suggests that the flow within the fan heater is turbulent. This information is critical for selecting appropriate turbulence models within the CFD software.

V.2. Geometry Description

The geometry of the fluid domain of the fan heater was developed in CATIA V5 (see figure 15).

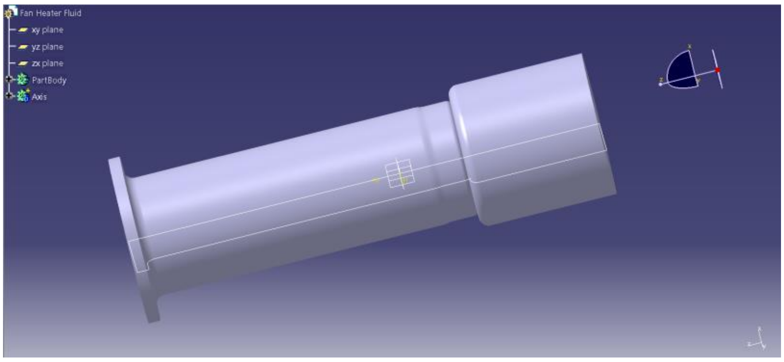

Figure 15: Geometry of the fluid domain of the fan heater on CATIA V5

This geometry encompasses a porous region, a honeycomb structure, and an exit. The porous region represents areas with complex internal details and unknown structures. The honeycomb structure replicates the actual device design. This geometry ensures the simulation results closely resemble real-world performance.

As shown in figure 16, the geometry was imported into ANSYS as an STP file. Specific regions were assigned named selections to define boundary conditions and properties in the simulation.

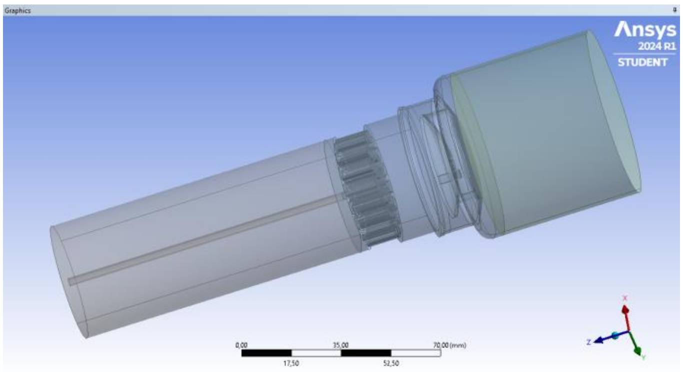

Figure 16: Geometry of the fluid domain of the fan heater imported to ANSYS Fluent

The geometry was segmented at the honeycomb part and exit part, to give us three fluid bodies; the porous body, the honeycomb geometry, and the exit. This segmentation will facilitate the meshing and the setup of the simulation.

Several named selections were assigned as the figure 17 illustrates.

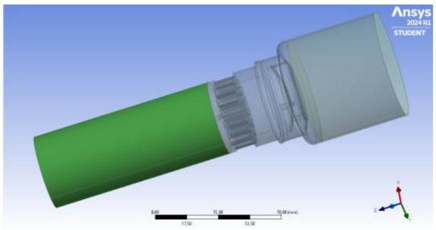

Porous exterior wall

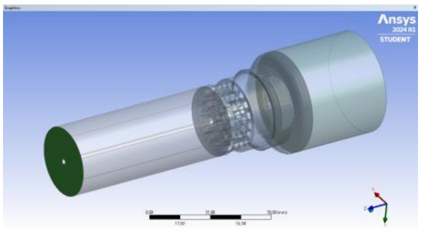

Mass inlet

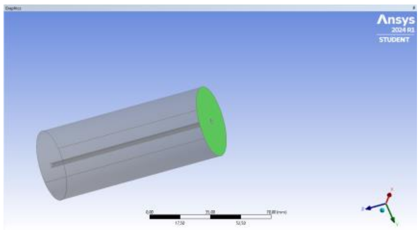

Interface porous-honeycomb

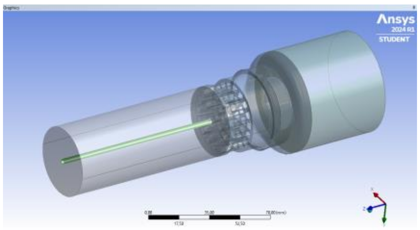

Interior porous wall

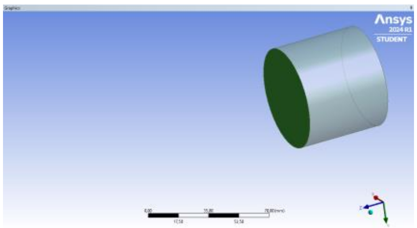

Interface exit-honeycomb

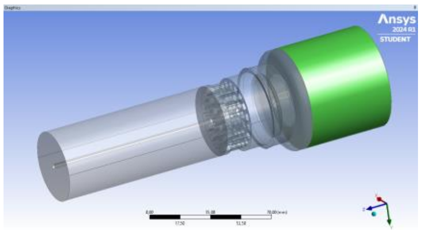

Exit wall

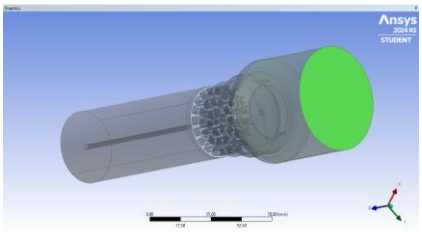

Outlet

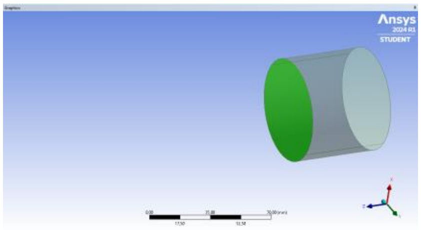

Interface honeycomb-exit

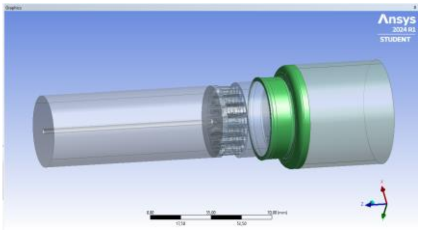

Wall honeycomb up

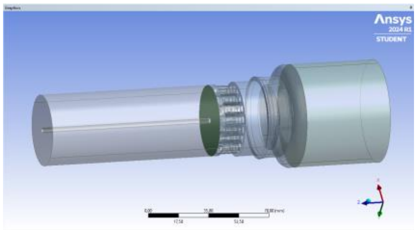

Interface honeycomb-porous

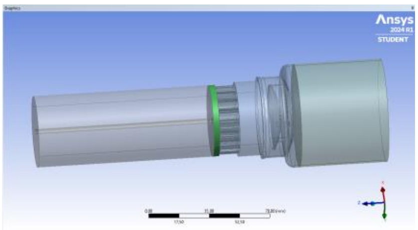

Wall exterior honeycomb

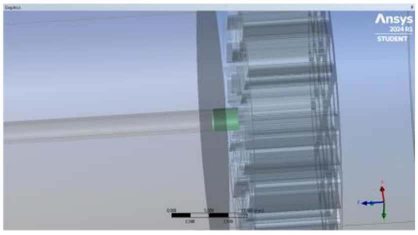

Wall interior honeycomb

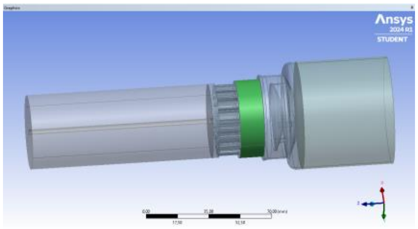

Wall honeycomb down

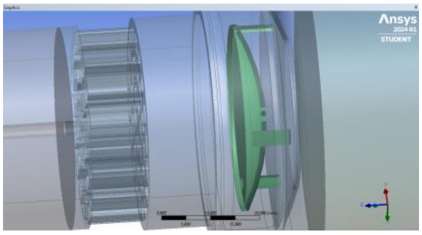

Conic wall

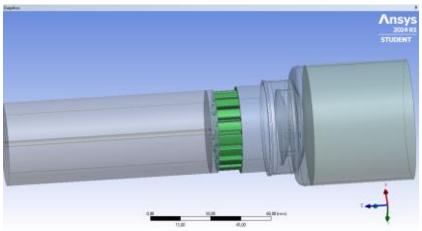

Wall honeycomb

Figure 17: The named selections used for the geometry

V.3. Description of the meshing parameters

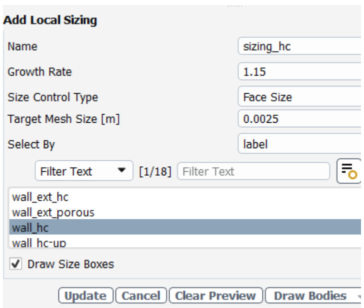

Local sizing 1

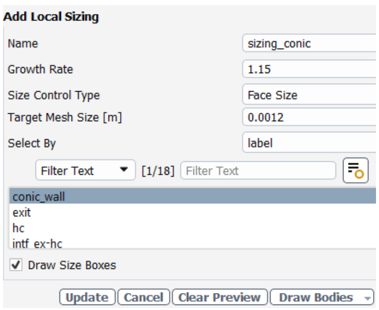

Local sizing 2

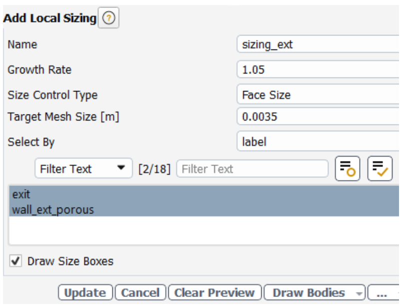

Local sizing 3

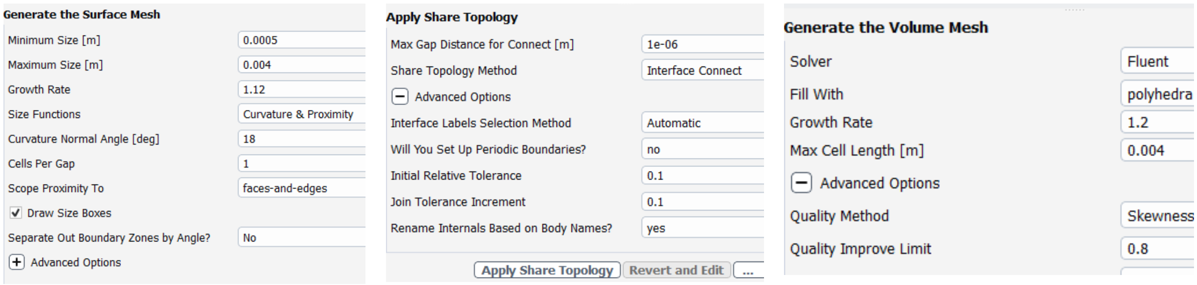

Creating surface mesh Share topology Generating volume mesh

Figure 18: Parameters used for meshing

The meshing process employed a combination of local sizings. These were applied to refine the mesh around the honeycomb wall and conic wall due to the expected high-velocity gradients in those regions. The minimum and maximum surface mesh sizes were set to 0.0005m and 0.004m, respectively, with a growth rate of 1.12. The « share topology » option was used to ensure mesh conformity across interfaces. The volume mesh consisted of polyhedral cells with a growth rate of 1.2 and a maximum cell length of 0.004m. This type of mesh was used as it offers good balance between accuracy and efficiency and works well for complex geometries. The parameters used are illustrated in Figure 18.

The display of the mesh, after, generating the volume mesh, is shown in figure 19.

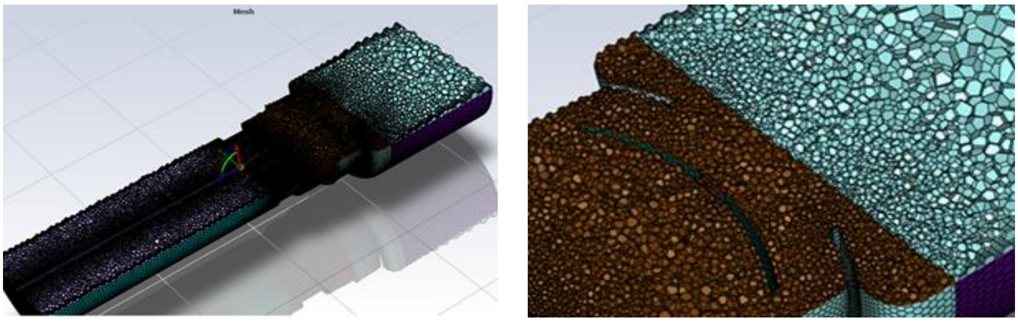

Figure 19: Mesh of the fan heater

V.4. CFD Setup

The next step is as shown in figure 20, the setup of the simulation.

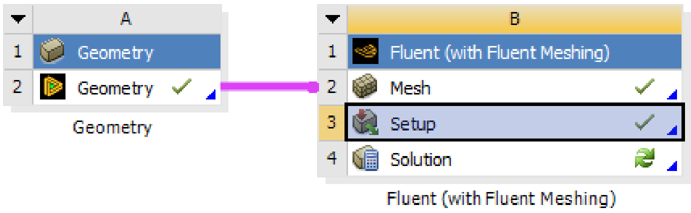

Figure 20: Workbench display

Solver:

A density-based solver was chosen for the simulation. This solver type is suitable for problems involving compressible flows.

The simulation was configured for steady conditions as the flow characteristics within the domain are assumed to remain constant over time. This is because the fan operated at its maximum speed; a fixed speed, and the operating conditions are assumed to be constant (see figure 21).

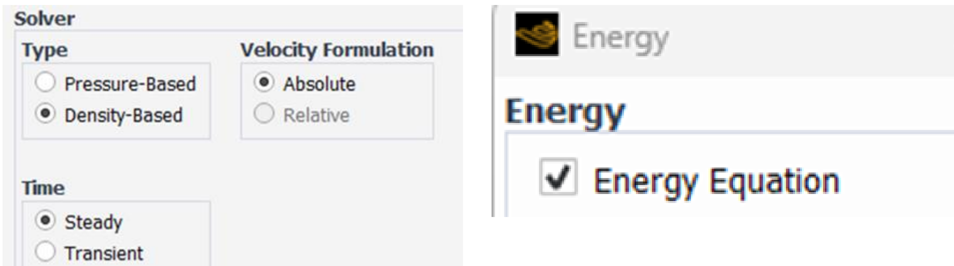

Figure 21: Solver type and energy equation

Turbulence model:

The standard k-ε turbulence model was implemented to account for the effects of turbulence on the flow. This model offers a balance between accuracy and computational cost. It solves transport equations for the turbulent kinetic energy (k) and the turbulent dissipation rate (ε) to capture the influence of turbulence on the flow behavior. (see figure 22)

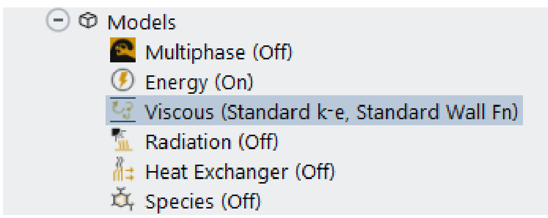

Figure 22: Turbulence models

Material properties:

Air was defined as the working fluid. The ideal gas model was employed to represent its behavior. This model assumes air behaves like a perfect gas, since the fan heater will operate at moderate air pressures.

Steel was selected as the solid material for the fan heater structure.

Operating conditions :

As the figure 23 shows, a reference pressure of 101325 Pa was set for the simulation, representing the atmospheric pressure surrounding the fan heater, it is located at the outlet (z=-0.085).

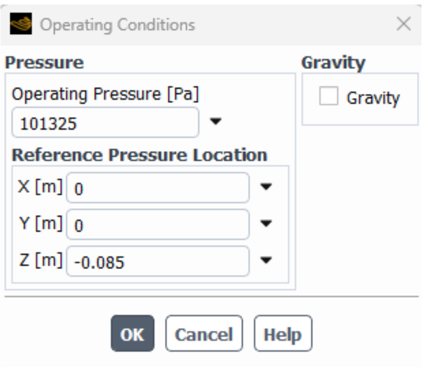

Figure 23: Operating conditions

Boundary conditions

Two primary boundary conditions were employed in the simulation :

- Mass Flow Inlet: This boundary condition was applied at the inlet of the fan heater. It specifies the mass flow rate of air entering the domain, due to the presence of the fan, at 0.0077kg/s, as calculated previously. Additionally, the maximum static pressure given by the manufacturer is 3500 Pa, representing the pressure drop. This value was defined in this simulation as the inlet. The initial temperature of the air entering the domain was specified as 298.15 K.
- Pressure Outlet: This boundary condition was applied at the outlet of the fan heater domain. It defines the pressure at which the air exits the system. A gauge pressure of 0.01Pa relative to the reference pressure was set at the outlet. The temperature of the air exiting the domain is 306.15 K.

The Figure 24 below presents the boundary condition parameters.

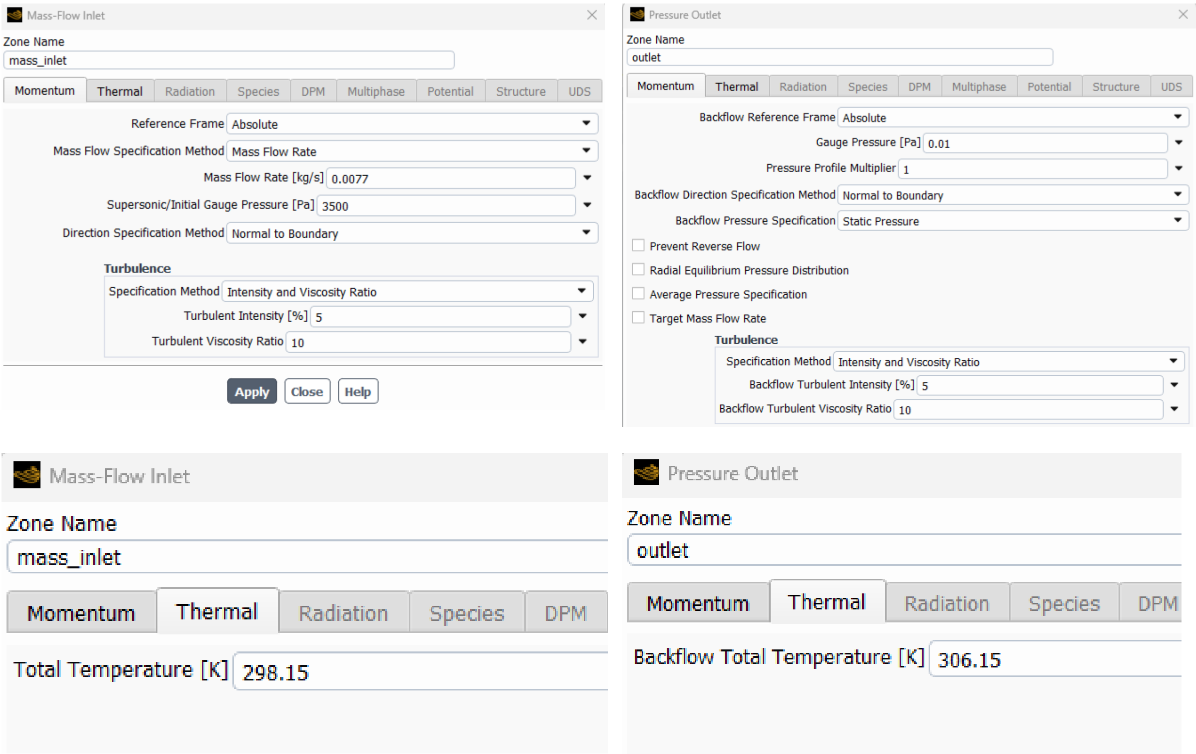

Figure 24: Boundary conditions

Initialization and iterations :

A hybrid initialization method was employed. A user-specified fluid time scale of 0.0001s was defined to improve convergence behavior. The simulation was run for a total of 2500 iterations (see figure 25).

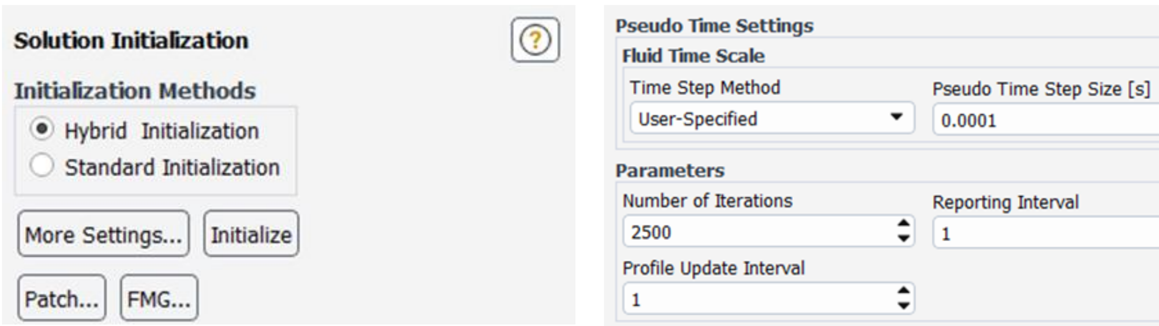

Figure 25: Initialisation and iterations

V.5. Results and Discussion

The simulation results revealed key insights into the flow behavior within the fan heater.

Contour of Z-velocity at the outlet

The first result focused on the Z-component of the velocity at the outlet (see figure 26). The contour of velocity demonstrated a high velocity at the central region with a magnitude of -7.9m/s, surrounded by a lower velocity at the peripheral region with a velocity of -0.79m/s. The values are negative since the flow goes in the -Z direction due to the geometry's orientation.

This observation suggests that the airflow exiting the fan heater is not uniform. The central region experiences a stronger acceleration, potentially due to the fan's influence and its geometry. The lower peripheral velocity might indicate a backflow or recirculation of the flow near the edges of the outlet. This is significantly important because a uniform and well-distributed airflow is essential for optimal performance of a catalytic converter. Therefore, we need to strategically place the filter at the outlet, in order to achieve a more optimal flow profile for the catalytic converter.

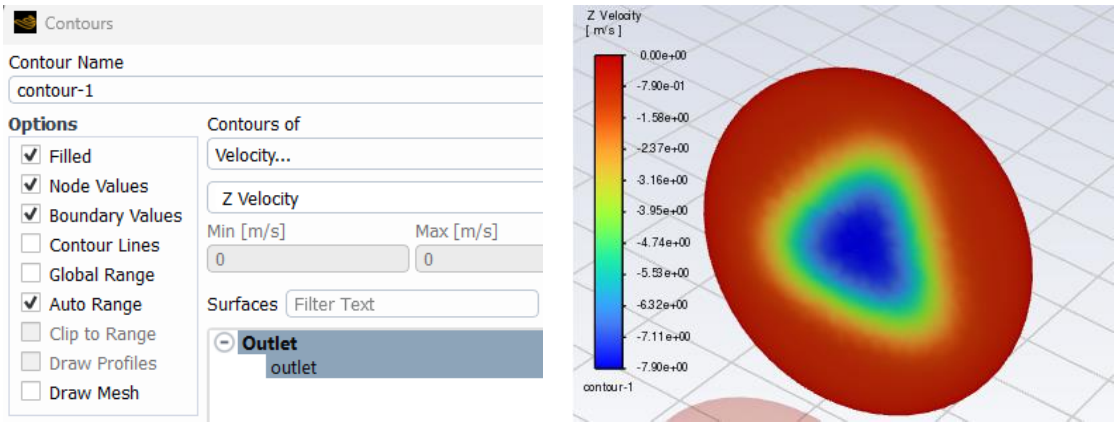

Figure 26: Contour of Z-velocity at the outlet of the device

Contour of velocity at a vertical line of the outlet

A vertical line plot at the outlet illustrated the velocity distribution. The color spectrum ranged from -9.99m/s to 4.01 m/s indicating a significant variation in the Z-component of velocity across the outlet plane.

Our experimental measurement at the center was -11m/s. Thus, this value is similar to the value visualized in the simulation. This is due to the precision and reliability of the experimental setup (see figure 27).

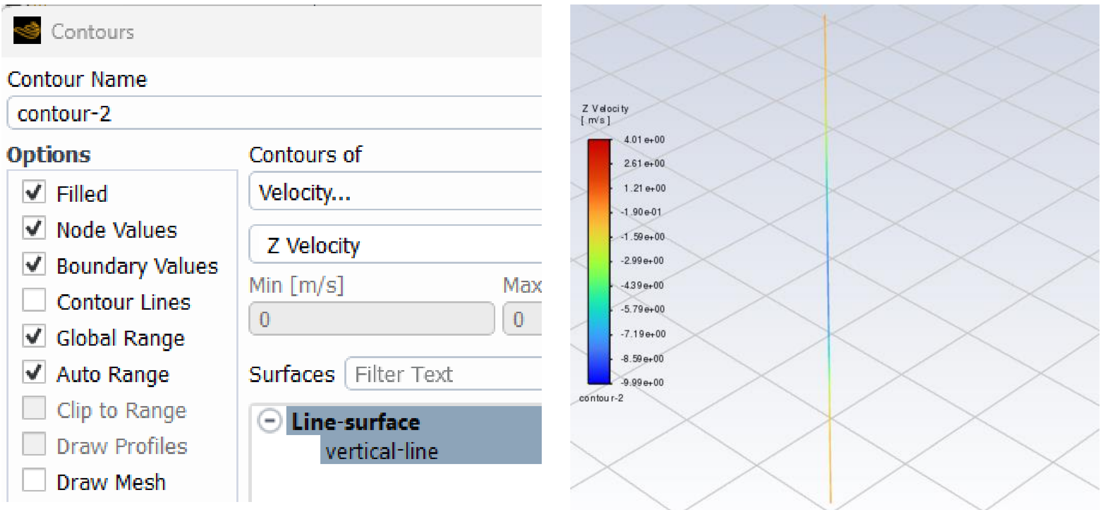

Figure 27: Contour of velocity at a vertical line of the outlet

Velocity vectors

Velocity vectors colored by velocity magnitude were visualized on walls, inlet, and outlet, as the figure 28 shows. This visualization described the overall flow pattern within the fan heater, with velocities ranging from 3.7 x 10^{-3} m/s to 11m/s. This helps us assess the effectiveness of the fan heater in achieving a desired airflow distribution within the domain.

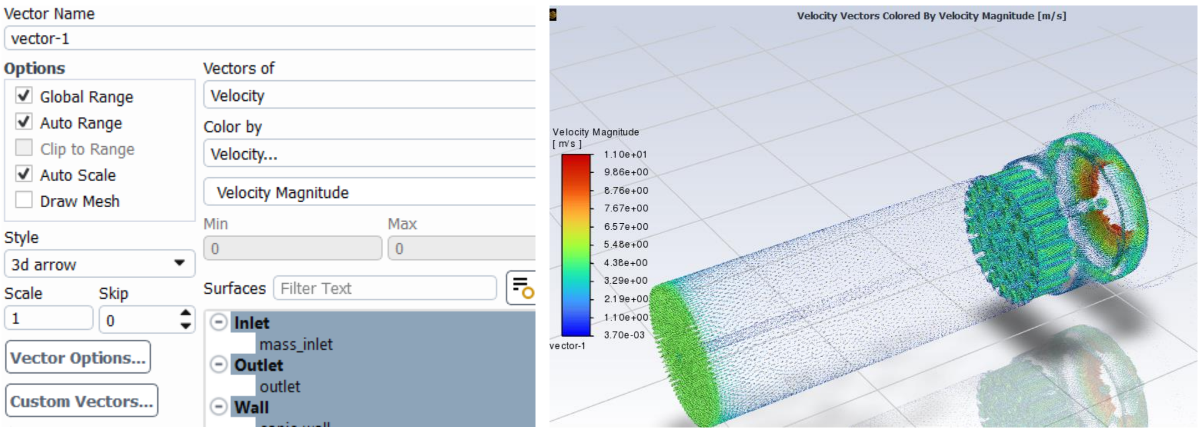

Figure 28: Velocity vectors

The “XY” plot shows the variation of the Z-component of velocity (Y-axis) along the length at a specific vertical line at the outlet (see figure 29). This path is represented by its curved length, which increases from 0 to 0.06 meters. The Z-velocity values range from -8 m/s to 0 m/s, with a negative sign due to the flow opposing the positive Z-axis, due to the geometry’s orientation.

The parabolic shape of the Z-velocity suggests a gradual change of velocity and acceleration along the path within the fan heater. The peak velocity is at X=0.03 meters, it indicates the point of the highest flow speed along this line.

XY plot

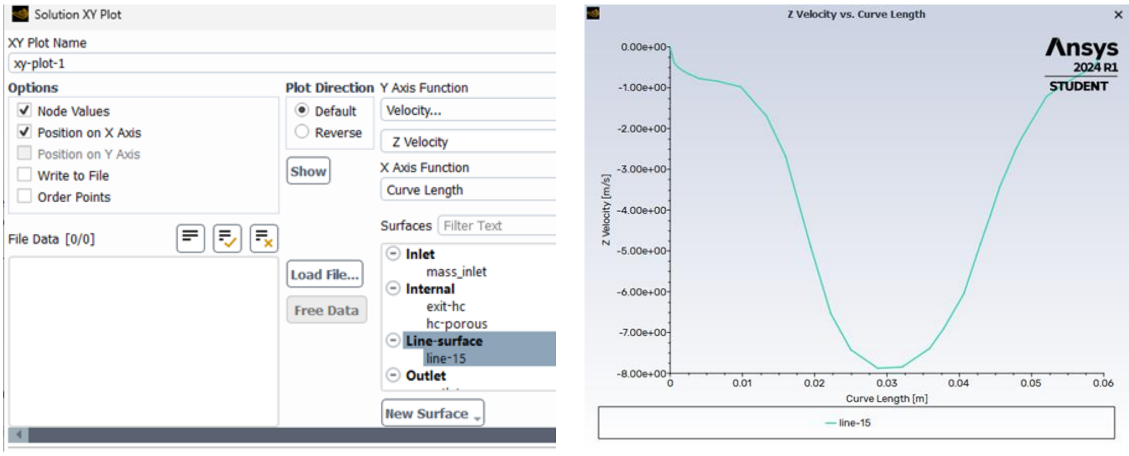

Figure 29: xy plot

Contour of Static Pressure on the "YZ" plane

The simulation has also revealed information about the pressure distribution within the domain through the static pressure contour on the YZ plane (see figure 30).

The static pressure is the highest at the inlet of the porous region, around 90 Pa. This indicates that the air entering the fan heater experiences a significant pressure increase, due to the fan's action.

The static pressure gradually decreases as the flow progresses through the porous region, honeycomb structure, and towards the outlet. This pressure drop is expected as the air encounters resistance within the geometry. The pressure values range from 71.4 Pa to 40.5 Pa in the honeycomb region, suggesting a continuous decrease in pressure.

A more significant pressure drop occurs just before the exit. The static pressure drops from around 40.5 Pa to 25.1 Pa.

The static pressure near the exterior tube and extending towards the outlet ranges from -1.15 Pa to 0.39 Pa. This is due to the flow exiting the confined space.

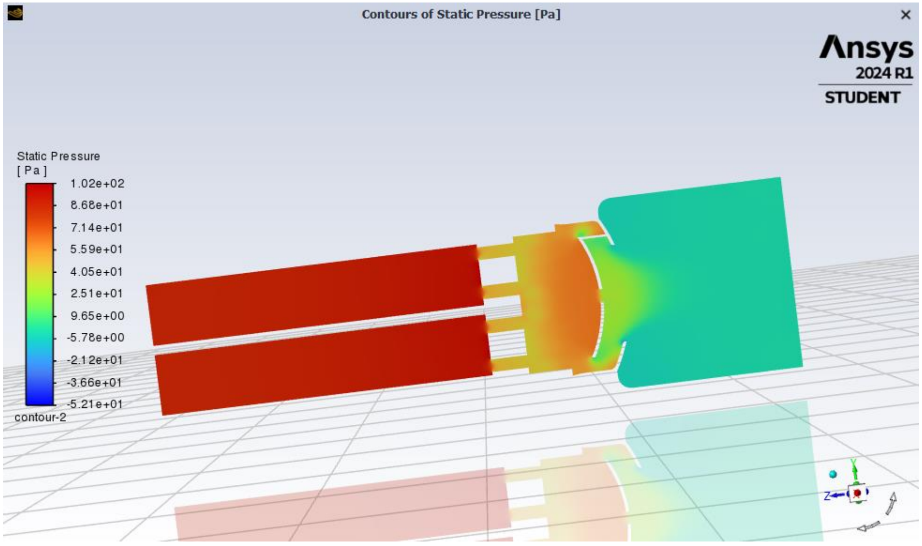

Figure 30: Contour of Static Pressure on the "yz" plane

Conclusion

The CFD simulation has provided valuable insights into the flow behavior and the pressure distribution within the fan heater. The analysis revealed that the velocity distribution at the outlet exhibits non-uniformity with a central high-velocity zone. This non-uniformity lead to uneven flow exiting the fan heater, potentially impacting the performance of the catalytic converter.

The pressure distribution analysis indicated a significant pressure drop throughout the domain. It is due to frictional losses between the air and the solid elements within the fan heater, such as the calls, porous media, or the honeycomb structure.

This highlights the importance of considering internal flow behavior when simulating a fan heater's performance. The observed non-uniformity in the velocity distribution suggests the need for potential design modifications to achieve a more even airflow exiting the tube and entering the catalytic converter.

General Conclusion

This project has explored the critical role of airflow parameters in automotive design. It has focused on wind tunnels, catalytic converters, and the application of CFD simulations.

The research presented in this work highlights the vital role of wind tunnels in evaluating airflow parameters around objects.

Furthermore, the study explored the importance of mesh generation in CFD simulations for accurately capturing airflow phenomena. Meshing methods and mesh quality were demonstrated to be essential for obtaining reliable results when simulating airflow patterns around vehicles.

The materials and methods employed in the research provided a framework for investigating the airflow parameters.

The CFD simulation of the fan heater revealed key findings about flow behavior and pressure distribution. The analysis identified non-uniformity in the velocity distribution. This uneven flow could potentially impact the performance of the catalytic converter. This research has served as a testament to the effectiveness of CFD simulations in uncovering flow phenomena within complex systems.

One potential solution to achieve a more even airflow exiting the fan heater would be the implementation of a flow conditioning device; the filter. This helps dampen flow fluctuations and promote a more uniform velocity profile at the outlet.

References :

[1] Yuxiang Zhang, Philip Cardiff, and Jennifer Keenahan. Wind-Induced Phenomena in Long-Span Cable-Supported Bridges: A Comparative Review of Wind Tunnel Tests and Computational Fluid Dynamics Modelling.

[2] Deepti Soni, Bhupendra Singh, Sanjeev Kumar Gupta, Vijay Kumar Dwivedi. Wind Tunnel: A Research Tool

[3] Frank M. White. Fluid Mechanics.

[4] Mrinal Kaushik. Theoretical and experimental aerodynamics.

[5] Surjatin Wiriadidijaja et al. Basic Geometries of the New Closed Circuit Wind Tunnel of the Universiti Putra Malaysia.

[6] John Kaiser Calautit et al. A Validated Design Methodology for a Closed Loop Subsonic Wind Tunnel.

[7] Nguyen Quoc Y. Designing, constructing, and testing a low-speed open-jet Wind Tunnel.

[8] SAHITH REDDY MADARA, JERRIN THADATHIL VARGHESE, and Dr. CHITHIRAI PON SELVAN Design And Fabrication of Cost Open Circuit Subsonic Wind Tunnel.

[9] https://encyclopedia2.thefreedictionary.com/wind+tunnel.

[10] Milliken, Douglas L, and William F Milliken. Race Car Vehicle Dynamics. Society of Automotive Engineers, Inc., 1995.

[11].www.globalspec.com/learnmore/labware_test_measurement/product_materiial_testing/wind_tunnels.

[12] S.M.Gorlin and I.I.Slezinger. Wind Tunnels and their instrumentation.

[13] Vinayak Shukla, Prof. Yogesh Tembhurne. A Review on Performance Enhancement of Catalytic Converter by Making Geometrical Changes, 2018.

[14] K. Sathish Kumar, V. Chandramohan. Design and Analysis of Catalytic Converter Using Computational Fluid Dynamics (CFD).

[15] Chirag Amin and Pravin P. Rathod. CATALYTIC CONVERTER BASED ON NON-NOBLE MATERIAL.

[16] Emmy Kritsanaviparkporn, Francisco M.Baena-Moreno and T.R.Reina. Catalytic Converters for Vehicle Exhaust: Fundamental Aspects and Technology Overview for Newcomers to the Field.

[17] Sohel Khalil Shaikh et al. An investigation of Three-Way Catalytic Converter for Various Inlet Core Angles Using CFD.
[18] Prof. (Dr.) Govind Chandra Mishra. Strategic Technologies of Complex Environmental Issues, Sustainable Approach.
[19] Anupam Mukherjee et al. Catalytic Converter in Automobile Exhaust Emission.
[20] N. Shimoda et al. Catalytic performance enhancement by heat treatment of $CuFe_2O_4$ spinel and γ-alumina composite catalysts for steam reforming of dimethyl ether.
[21] ANSYS Fluent User's Guide (2023). ANSYS Inc.
[22] P.Singh, A. Kumar and K.K. Khatua. Concept of Turbulence Modelling and Its Application in Open Channel Flow.

[23] Joe F. Thompson, Bharat K. Soni, Nigel P. Weatherill. Handbook of Grid Generation.

[24] Joel Guerrero. Introduction to Computational Fluid Dynamics: Governing Equations, Turbulence Modeling Introduction and Finite Volume Discretization Basics.

[25] Sujit Shedage. Numerical investigation of micro-scale flows in narrow gaps.

[26] H K Versteeg and W Malalasekera. An Introduction to Computational Fluid Dynamics.

[27] Patrick J.Roache. Verification and Validation in Computational Science and Engineering. Hermosa Publishers.

[28] J.H. Ferziger and M. Peric. Computational Methods for Fluid Dynamics.